AD-A168 908 OPTICAL PHASE CONJUGATION VIA FOUR-WAVE MIXING IN BARIUM TITANATE(U) NAVAL POSTGRADUATE SCHOOL MONTEREY CA J R RYAN MAR 86 1/1

UNCLASSIFIED F/G 20/6 NL

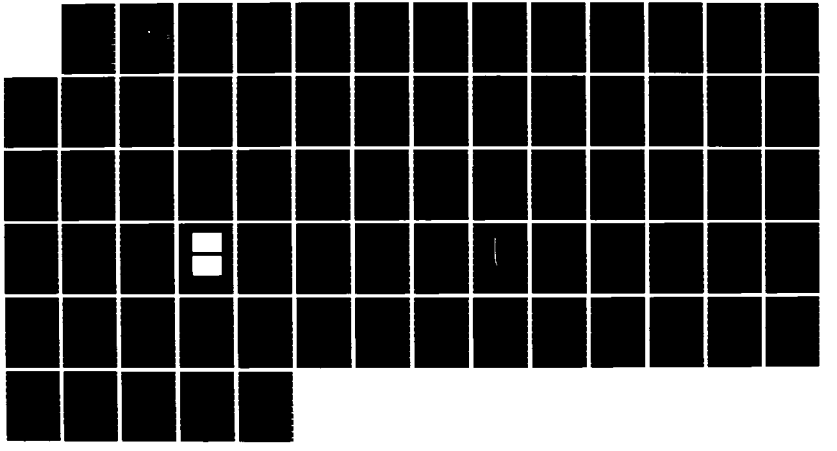

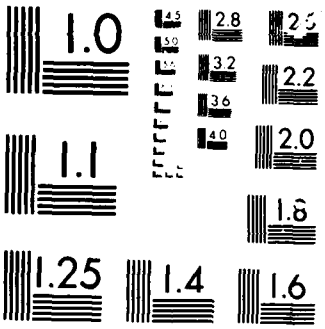
1.0
1.1
1.25
1.4
1.6
1.8
2.0
2.2
2.8
3.2
3.6
4.0

NAVAL POSTGRADUATE SCHOOL
Monterey, California

THESIS

OPTICAL PHASE CONJUGATION
VIA FOUR-WAVE MIXING IN BARIUM
TITANATE

by

James Roger Ryan

March 1986

Thesis Advisor: D. L. Walters

Approved for public release; distribution is unlimited.

SECURITY CLASSIFICATION OF THIS PAGE

REPORT DOCUMENTATION PAGE

1a REPORT SECURITY CLASSIFICATION	1b RESTRICTIVE MARKINGS
2a SECURITY CLASSIFICATION AUTHORITY	3 DISTRIBUTION / AVAILABILITY OF REPORT Approved for public release; distribution is unlimited.
2b DECLASSIFICATION / DOWNGRADING SCHEDULE	
4 PERFORMING ORGANIZATION REPORT NUMBER(S)	5 MONITORING ORGANIZATION REPORT NUMBER(S)
6a NAME OF PERFORMING ORGANIZATION: Naval Postgraduate School 6b OFFICE SYMBOL (If applicable): 61	7a NAME OF MONITORING ORGANIZATION: Naval Postgraduate School
6c ADDRESS (City, State, and ZIP Code): Monterey California 93943-5000	7b ADDRESS (City, State, and ZIP Code): Monterey California 93943-5000
8a NAME OF FUNDING / SPONSORING ORGANIZATION 8b OFFICE SYMBOL (If applicable)	9 PROCUREMENT INSTRUMENT IDENTIFICATION NUMBER
8c ADDRESS (City, State, and ZIP Code)	10 SOURCE OF FUNDING NUMBERS PROGRAM ELEMENT NO / PROJECT NO / TASK NO / WORK UNIT ACCESSION NO

11 TITLE (Include Security Classification)
OPTICAL PHASE CONJUGATION VIA POUR-WAVE MIXING IN BARIUM TITANATE

12 PERSONAL AUTHOR(S)
Ryan, James R.

13a TYPE OF REPORT	13b TIME COVERED	14 DATE OF REPORT (Year, Month, Day)	15 PAGE COUNT
Master's Thesis	FROM _____ TO _____	March 1986	72

16 SUPPLEMENTARY NOTATION

17 COSATI CODES			18 SUBJECT TERMS (Continue on reverse if necessary and identify by block number)
FIELD	GROUP	SUB-GROUP	Nonlinear Optics, Optical Phase Conjugation, Four-wave Mixing, Distortion Correction

19 ABSTRACT (Continue on reverse if necessary and identify by block number)

Photorefraction in a crystal of barium titanate can produce a phase conjugate replica of a laser beam through four-wave mixing. Barium titanate is unique because self generated conjugate returns will form from corner reflections. Self pumped optical phase conjugation was achieved at six wavelengths between 457.9 and 514 nm. Factors affecting the return included the laser wavelength, intensity, and angle of incidence with the c axis. The average return amounted to about 25% of the incident beam. The phase conjugate return interacted with the laser modes, significantly increasing the laser power.

20 DISTRIBUTION / AVAILABILITY OF ABSTRACT	21 ABSTRACT SECURITY CLASSIFICATION
☒ UNCLASSIFIED/UNLIMITED ☐ SAME AS RPT ☐ DTIC USERS	Unclassified
22a NAME OF RESPONSIBLE INDIVIDUAL: D. L. Walters	22b TELEPHONE (Include Area Code): 408-646-2486 / 22c OFFICE SYMBOL: 61

DD FORM 1473, 84 MAR 83 APR edition may be used until exhausted
All other editions are obsolete

SECURITY CLASSIFICATION OF THIS PAGE

Approved for public release, distribution unlimited

Optical Phase Conjugation via Four-wave Mixing in Barium Titanate

by

James Roger Ryan
Lieutenant, United States Navy
B.S., Oregon State University

Submitted in partial fulfillment of the requirements for the degree of

MASTER OF SCIENCE IN PHYSICS

from the

NAVAL POSTGRADUATE SCHOOL
March 1986

Author: James R. Ryan
James R. Ryan

Approved by: Donald L. Walters
Donald L. Walters, Thesis Advisor

Alfred W. Cooper
Alfred W. Cooper, Second Reader

Gordon E. Schacher
Gordon E. Schacher, Chairman,
Department of Physics

John N. Dyer
John N. Dyer, Dean of Science and Engineering

ABSTRACT

Photorefraction in a crystal of barium titanate can produce a phase conjugate replica of a laser beam through four-wave mixing. Barium titanate is unique because self generated conjugate returns will form from corner reflections. Self pumped optical phase conjugation was achieved at six wavelengths between 457.9 and 514 nm. Factors affecting the return included the laser wavelength, intensity, and angle of incidence with the c axis. The average return amounted to about 25% of the incident beam. The phase conjugate return interacted with the laser modes, significantly increasing the laser power.

TABLE OF CONTENTS

I. INTRODUCTION

Optical phase conjugation is a nonlinear optical phenomenon that replicates a distorted electromagnetic wave. This process has potential in distortion correction, pointing and tracking, improved laser resonators, image enhancement, and optical communications. Nonlinear effects that can produce a phase conjugate wave include: photorefraction, Brillouin scattering, Raman scattering, Kerr-like four-wave mixing, photon echoes, three wave mixing, and electrostrictive effects. Some of the most promising results have come through the use of photorefractive crystals such as $LiNbO_3$, $BaTiO_3$, $KNbO_3$, and $Bi_{12}SiO_{20}$. These crystals provide phase conjugate reflection at milliwatt power levels, and much more easily than other materials. The biggest difficulty in working with these crystals is obtaining one. Production is difficult, slow, and only a fraction of the crystals produced are optically active. $BaTiO_3$ was chosen for these experiments because of its high sensitivity, diffraction efficiency, and availability.

This thesis identifies those parameters that affect the speed and performance of phase conjugation in barium titanate, by measuring the effect of power, frequency, and angle of the incident beam.

II. THEORY

A. PHASE CONJUGATION

Optical phase conjugation is the process of creating the complex conjugate of an electromagnetic wave. The phase of the electric field component **E** can be described by [Ref. 1]

$$\mathbf{E}_1(\mathbf{r},t) = \Phi(\mathbf{r})\exp[i(wt-\mathbf{k}\cdot\mathbf{r})]. \quad (1)$$

The complex conjugate of this wave is then

$$\mathbf{E}_2(\mathbf{r},t) = \Phi^*(\mathbf{r})\exp[i(-wt+\mathbf{k}\cdot\mathbf{r})]. \quad (2)$$

Yariv summarizes the important application aspects of phase conjugation in his Distortion Correction Theorem.

> If a (scalar) wave $E_1(\mathbf{r})$ propagates from left to right through an arbitrary dielectric (but lossless) medium, then if we generate in some region of space (say near z=0) its phase conjugate replica $E_2(\mathbf{r})$ then E_2 will propagate backward from right to left through the dielectric medium remaining everywhere the phase conjugate of E_1. [Ref. 2: p. 500]

The proof of this follows from the properties of the wave equation. E_1 obeys

$$\nabla^2 E_1 + w^2\mu\epsilon(\mathbf{r})E_1 = 0, \quad (3)$$

where $\epsilon(\mathbf{r})$ includes any contributions from distortion effects. Using the expression for the electric field given in equation (1)

$$\nabla^2\Phi_1 + [w^2\mu\epsilon(\mathbf{r})-k^2]\Phi_1 - 2ik(\Phi_1) = 0. \quad (4)$$

The complex conjugate of this is

$$\nabla^2\Phi_1^* + [w^2\mu\epsilon^*(\mathbf{r})-k^2]\Phi_1^* + 2ik(\Phi_1^*) = 0. \quad (5)$$

Starting instead with E_2 the wave equation (3) is

$$\nabla^2\Phi_2 + [w^2\mu\epsilon(\mathbf{r})-k^2]\Phi_2 + 2ik(\Phi_2) = 0. \quad (6)$$

If $\epsilon(\mathbf{r}) = \epsilon^*(\mathbf{r})$, which is true for a lossless (and gainless) medium, then equations (5) and (6) for Φ_1^* and Φ_2 are identical. Since Φ_1 and Φ_2 are solutions to the same second order linear differential equation, they are equal to within an arbitrary constant.

There are several properties of optical phase conjugation that have important consequences for applications. The first is that phase conjugation reverses both the direction of propagation and the phase factor of the electromagnetic wave. This causes the light to retrace its path, and as such has been referred to as a "perfect mirror". Ordinary mirrors reverse the sign of only the normal component of the propagation vector **k**, causing light to reflect so that the angle of incidence equals the angle of reflection. A phase conjugate mirror (PCM) reverses both the normal and transverse components of **k**, causing light to come back along the direction of incidence. Changing the orientation of a phase conjugate mirror will not affect the direction at which light is "reflected". This property is illustrated in Figure 1.

Because the reflection from a PCM returns along the direction of incidence, it will retrace the incident path. If the direction of propagation had been redirected between the source and the PCM by, for example, a prism, the light would return through the prism to the source. Any arbitrary

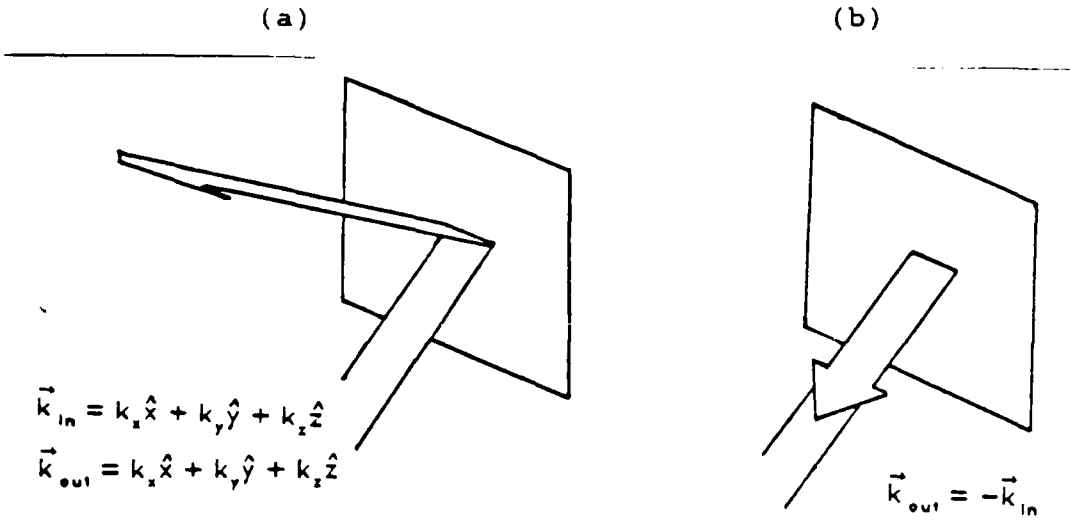

Figure 1. (a) Ordinary Mirror (b) Phase Conjugate Mirror [Ref. 3: p. 3]

distortion in direction along the path of propagation can be thought of as a series of appropriately placed prisms, directing the light to the source.

The phase of the PCM reflected wave is the complex conjugate of the incident electric field. Therefore the wavefront of the backward travelling light is everywhere identical to the incident light. A nonuniform portion of the medium that imposes a phase distortion or delay on the wavefront between the source and the PCM, would be traversed in the opposite direction on the return trip, returning the wavefront to its original condition (see Figure 2).

This distortion correction property of phase conjugation is similar to a "time reversal" of the light beam. However, this analogy is not exact. Losses in propagation and in the

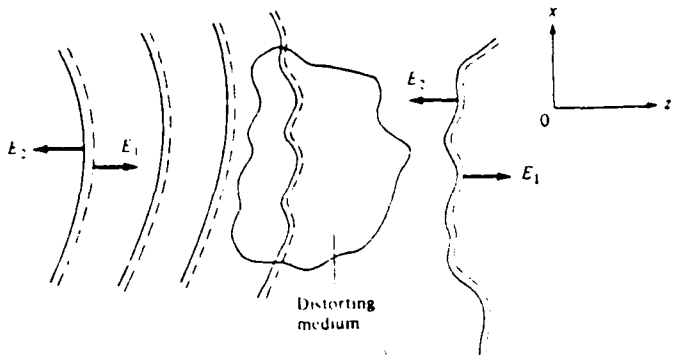

Figure 2. Distortion Correction of a Wavefront
[Ref. 2: p. 500]

phase conjugation process will reduce the amplitude of the return beam. Also, diffraction must be taken into account. (Losses in amplitude can be corrected by a process known as two beam coupling which will be discussed later.)

Another property of phase conjugation that has important consequences is that it occurs rapidly. Once the phase grating has been established, which takes only a few seconds, the PCM can continuously respond to dynamic changes. This means that the distortion correction properties can be used directly, without a processing delay such as chemical development for a conventional hologram.

B. NONLINEAR OPTICAL EFFECTS

Phase conjugation is the result of a nonlinear response in the phase conjugate medium to the electric field of the electromagnetic wave. In a nonlinear medium

$$\nabla^2 \mathbf{E} - \mu_o \epsilon (\delta^2 \mathbf{E}/\delta t^2) = \mu_o (\delta^2 \mathbf{P}/\delta t^2), \quad (7)$$

where **P** represents the nonlinear portion of the polarization vector. In a linear medium this reduces to the more familiar form of the wave equation. The right hand term allows coupling and production of electromagnetic waves in the medium.

The electric field dependent susceptibility X(E) is given by [Ref. 3: p. 11]

$$X(E) = X^{(1)} + X^{(2)}E + X^{(3)}E^2 + \ldots . \quad (8)$$

The polarization is then given by

$$\mathbf{P}(E) = EX(E) = X^{(1)}E + X^{(2)}E^2 + X^{(3)}E^3 + \ldots . \quad (9)$$

The linear term ($X^{(1)}$) produces gain, absorption, index of refraction, and birefringence. The second order term leads to the Pockels effect, second harmonic generation, parametric mixing, and frequency addition and subtraction. The third order term allows third harmonic generation, Raman scattering, stimulated Brillouin scattering, three wave mixing, degenerate and nondegenerate four wave mixing, and Kerr and Kerr-like effects. All of the above nonlinear effects, as well as others such as electrostrictive effects in aerosols, can produce phase conjugate waves. [Ref. 1: p 7]

This thesis will concentrate on third order Kerr-like effects. For these effects, the index of refraction, and therefore the speed of light, depends on the intensity of the light in the medium. This can be represented by [Ref.

3: p. 14]

$$n = n_o + n_2 \langle E^2 \rangle, \qquad (10)$$

where the brackets represent the temporal average. If the light intensity varies in time, so will the index of refraction, and a pulse of light will experience a time-varying index of refraction, known as self-phase modulation. If there are multiple beams in the medium, the refractive index at each point will depend on the net intensity at that point.

There are two classes of Kerr-like effects. The first is the actual Kerr effect in which the change in refractive index of a material depends on the local field intensity (i.e. on the square of the electric field at that point). The second is the class of effects in which the change in refractive index depends on nonlocal fields (i.e. on fields that are not a maximum at the point of maximum change in index of refraction). The physical effects responsible for the second class include the following: thermal effects in materials having a temperature dependent index of refraction, in which exposure to light yields a temperature gradient causing a spatial modulation of the index; electrostrictive effects, in which the electric field gradient perturbs the density of nonabsorbing scattering centers, spatially modulating the index; and photorefractive effects. Feinberg summarizes photo-refraction as follows:

> Light causes charge to migrate and separate in a crystalline material. The separation of charge produces a

> strong electrostatic field, on the order of 10^5 V/m. The electrostatic field causes a change in the refractive index of the crystal by the linear electro-optic effect (the Pockels effect). [Ref. 3: p. 418]

This migration can be due to diffusion, drift in an external field, or a bulk photovoltaic effect, and will be discussed in the next section. Photorefractive materials include $BaTiO_3$, $Bi_{12}SiO_{20}$ (BSO), and $LiNbO_3$.

C. PHOTOREFRACTION

In electro-optic crystals, the light-induced refractive index changes are due to the spatial modulation of photocurrents by *nonuniform* illumination [Ref. 4; p. 206]. At low light intensities, photocurrent generation is dependent on the presence of suitable charge donors in the material. The charges may be either electrons or holes. Donors or trapping centers are provided by small traces of impurities [Ref. 3: p. 419]. Iron impurities have been shown to be an important contributor in ferroelectric crystals [Ref. 5: p. 298], in conjunction with a balance of oxygen vacancies, through doping experiments [Ref. 6].

Upon absorption of the proper wavelength of light, holes or electrons will move until trapped at another location. Under nonuniform illumination, the charges will be reexcited in the illuminated regions until they move into a nonilluminated region and are trapped. Uniform illumination allows the charges to redistribute evenly and completely restores the crystal to its original state. Prolonged use

of these materials indicates that there is no sign of damage or discoloration.[Ref. 7: p. 12]

There are three physical processes for the transport of charges in crystals when exposed to light: diffusion; drift in external fields; and a bulk photovoltaic effect [Ref. 8: p. 817]. Which process is the dominant effect depends on the type of crystal. In general the space charge field is given by

$$\mathbf{E}_i(z) = -m'[(\mathbf{E}_{ph} + \mathbf{E}_{ex})^2 + \mathbf{E}_{diff}^2]^{1/2} \cos(Kz + \phi), \quad (11)$$

where

$$\phi = \arctan \mathbf{E}_{diff}/(\mathbf{E}_{ph} + \mathbf{E}_{ex}), \quad (12)$$

$$m' = m/(1 + \sigma_d/\sigma_l), \quad (13)$$

and

$$\mathbf{E}_{diff} = kTK/e. \quad (14)$$

$\mathbf{E}_{ph}$, $\mathbf{E}_{ex}$, and $\mathbf{E}_{diff}$ are the photovoltaic, external and diffusion fields, respectfully, K is the spatial frequency of the modulation = $2\pi/L$, L is the fringe spacing = $\lambda/(2\sin\theta)$, m is the modulation index, and σ_d and σ_l are the photo- and dark conductivities. The change in the refractive index is then

$$n = -(n^3 r/2\epsilon\epsilon_o)\, E_i, \quad (15)$$

where r is the corresponding electro-optic coefficient, and ϵ is the static dielectric constant.[Ref. 8: p. 817]

In the absence of light, the charges will redistribute themselves depending on the dark conductivity. The dark conductivity will also be present when the crystal is

illuminated, and acts to reduce the effectiveness of the charge separation. Low dark conductivity, suitable donors, and efficient charge migration are needed to obtain high photorefractive efficiency. The rate of charge migration can be influenced by a number of factors, including temperature, and direction and magnitude of applied electric field. The extent of each effect varies for each individual crystal, depending on the type of material and its specific impurity composition.

The intersection of two coherent light beams crossing at an angle in a crystal sets up an intensity interference pattern whose spatial frequency can be varied by changing the crossing angle of the two beams. Charges migrate from the light areas to the dark areas, creating an electric field, which in turn forms a refractive index grating through the Pockels effect. This is shown in Figure 3. The location of the maximum induced electric field does not correspond to the maximum of the intensity pattern, but is half way between the extremes. The maximum refractive index change will be shifted one quarter of the period of the intensity pattern, where the gradient in intensity is largest, justifying the term nonlocal response.

Because the materials used are of significant depth, the phase grating which is set up is three dimensional, extending throughout the crystal. Subsequent incident light interacts with the grating, permitting interference of the

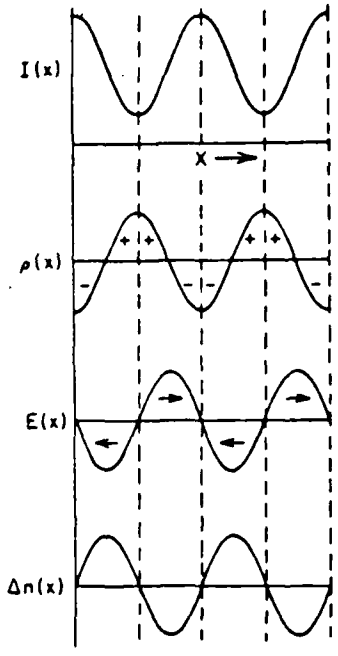

Figure 3. Photorefractive Index Grating Formation
[Ref. 3: p. 422]

incident beam with its own diffracted beam in the medium. There may be a phase shift with respect to the initial grating, so that the two beams interfere constructively or destructively, leading to a dynamic redistribution of the intensity pattern. There is a time factor inherent in the build up of the space-charge field, and the inertia of this nonlinear response prevents the phase shift between the light intensity pattern and the dynamic grating from realigning to a configuration in which there is no energy transfer.

The rate of creation and efficiency of the grating depends on several factors. Because the refractive index

change is proportional to the amount of charge moved, a certain optical energy must be deposited rather than a certain level of power. The absorption of the materials is generally too low to measure, but as an example, Feinberg estimates that several microjoules are required to write a high efficiency grating in $BaTiO_3$ [Ref. 7: p. 1297]. The time to deposit a given optical energy is inversely proportional to the intensity, so the speed of grating formation can be controlled by varying the intensity. As an example, again in $BaTiO_3$, creation times of a few seconds for 10^{-3} W/cm^2 to a few milliseconds for 1 W/cm^2 have been reported.[Ref 7: p. 1298] Recent experiments have shown that the grating formation rate is slightly less than linearly proportional to intensity, i.e. as I^x where $x = 0.6$ to 0.9 depending on the temperature and intensity range.[Ref. 9] Experimentally, longer wavelengths require longer time or a higher intensity to obtain the same results. Phase conjugation has been demonstrated (using a variety of materials) over the entire visible spectrum [Ref. 7: p. 1297] and as high as 1.06 μm [Ref. 10].

The amplitude of the grating distribution depends on the ratio of the periodic component of the intensity pattern to the uniform background intensity. The ratio of the periodic component to the uniform component is called the modulation index m. If the intensity of one of the beams is much greater than the other, the uniform component will dominate

and wash out the grating. Increasing the crossing angle between the beams at small angles reduces the period of the resulting field, and has been shown to increase the writing and erasing rates of the grating.[Ref. 7: p. 1298]

The diffraction efficiency of the grating in most materials is also dependent on the alignment of the resultant wave vector $\mathbf{k} = \mathbf{k}_1 - \mathbf{k}_2$ with the c axis of the crystal.[Ref. 3: p. 424] This is because the optical dielectric tensor is highly anisotropic.

The final factor in grating efficiency is the specific material used. Refractive index changes in response to the same stimulus vary widely. Also, the storage time of the grating depends on the dark current as

$$T_d = \epsilon\epsilon_o/\sigma_d . \qquad (16)$$

Values range from a few seconds for $KNbO_3$, to almost a year for $LiNbO_3$.[Ref. 7: p. 225]

D. BEAM INTERACTIONS

The phase shift between the light intensity maximum and the refractive index maximum is the primary factor in causing coupling between light beams in a phase conjugate medium. The first consequence of this shift is a process known as two beam coupling. This effect is illustrated in Figure 4. Two coherent beams intersect at an angle 2θ in the medium. The plane of incidence of the two beams is parallel to the c axis, and the bisector of the angle between the two beams is perpendicular to the c axis. This

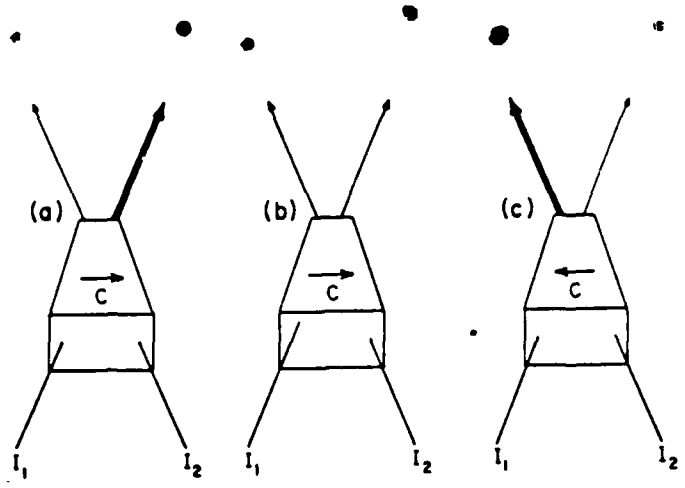

Figure 4. (a)Beams Intersect (b)Beams Do Not Intersect (c)C Axis Reversed [Ref. 3: p. 432]

maximizes the component of the resulting wave vector in the direction of the c axis. To maximize two beam coupling, the beams also should be polarized parallel to the c axis (i.e., horizontally polarized) so that the extraordinary ray will be used, taking advantage of the generally much larger component of the electro-optic tensor.

The two incident beams form an intensity pattern in the crystal that has maxima separated by $\lambda/2\sin\theta$, and minima half way between the maxima (see Figure 5). Each of the transmitted beams is the sum of two parts; the first order Bragg diffracted wave off the grating from one incident beam, and the zeroth order wave of the other (undiffracted) incident beam (see Figure 6). If the refractive index grating were unshifted, the diffracted beam would have a phase shift of $\pi/2$ relative to the undiffracted beam, and

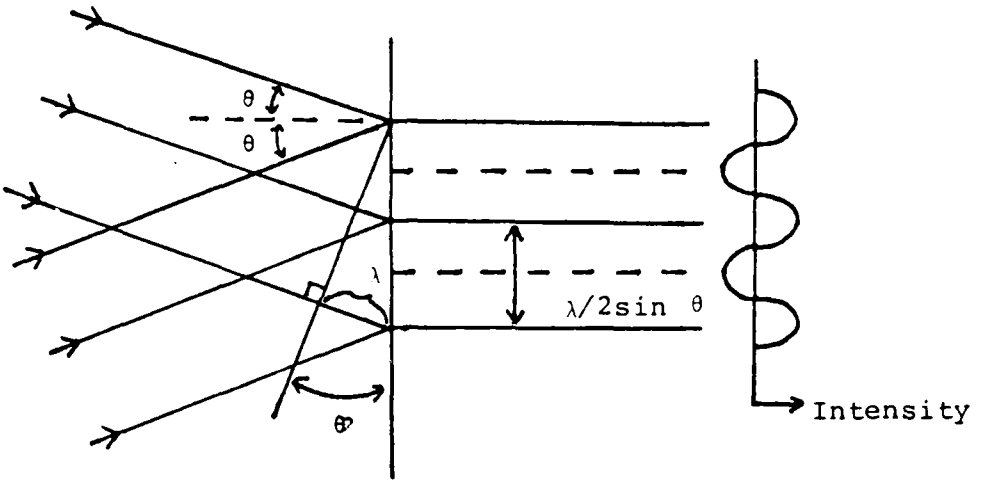

Figure 5. Intensity Pattern in the Crystal

energy transfer would be forbidden due to destructive interference [Ref. 4: p. 244]. However, with the grating shifted by a quarter of a period of the intensity pattern ($\lambda/8\sin\theta$), the diffracted beam experiences an additional

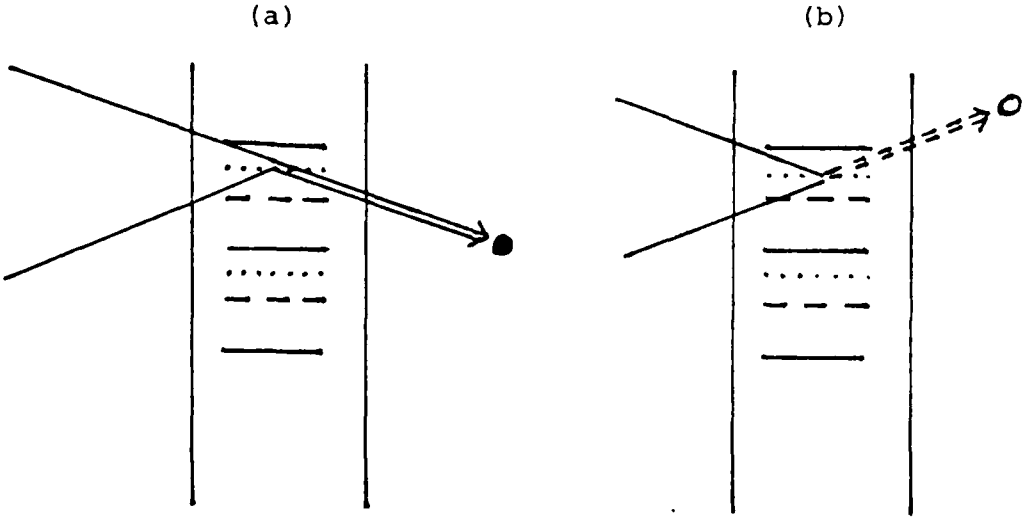

Figure 6. (a)Beam 1 Undiffracted, Beam 2 Diffracted
(b)Beam 1 Diffracted, Beam 2 Undiffracted

shift of $\pi/2$. The shift is due to the difference in path length between the diffracted and undiffracted beams. This shift is either $\pm \pi/2$ depending on whether the grating shifted towards or away from the diffracted beam. If the grating shifted towards the diffracted beam, the diffracted and undiffracted beams will constructively interfere. If the grating shifted away, they will destructively interfere. The result is a transfer of energy from one beam to the other. Since the grating shifts in the direction of the c axis, this may be used to determine the direction of the axis, and is a quick check on whether a crystal exhibits photo-refractive properties.

It is important to note that there is no transfer of energy if the beams do not intersect in the crystal, since no grating will form. If the crystal vibrates slightly, no energy will be transferred because the intensity pattern will not be stable long enough for the grating to form [Ref. 7: p. 1300]. It has been shown that phase information is not transferred to the other beam along with the energy, so there is no phase cross talk [Ref. 11: p. 621]. Thus two beam coupling can be used to boost the power of another coherent beam.

Another consequence of the grating phase shift, which is closely related to two beam coupling, is four wave mixing (FWM). It is used to produce a phase conjugate beam. In FWM (See Figure 7) two counterpropagating (colinear)

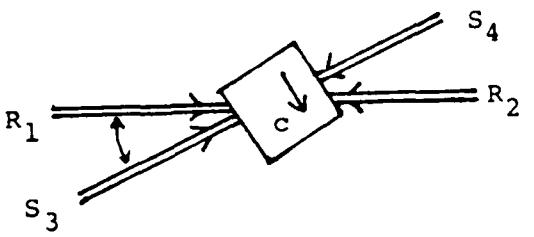

Figure 7. Four Wave Mixing Geometry
[Ref. 3: p. 421]

reference beams R_1 and R_2 pass through the crystal at an angle with the c axis. A third signal beam (the one to be conjugated) is then sent in at an angle 2θ with one of the reference beams. The appearance of the fourth wave can be thought of as the simultaneous writing and reading of two sets of gratings as follows. R_1 and S_3 produce a grating that diffracts R_2, generating S_4, which is the phase conjugate of S_3. At the same time, R_2 and S_3 produce a grating which diffracts R_1, also generating a contribution to S_4. This is shown in Figure 8. The phase conjugate beam of R_1 with R_2, and S_3 is then the sum of the two contributions. Once S_4 has been formed, it may undergo the same interactions with R_1 and R_2 as S_3, generating a contribution to the original signal beam. The interaction with S_4, does not need to be considered because Bragg diffraction of the other pair of beams will not occur, and because energy can not be transferred between opposite beams.

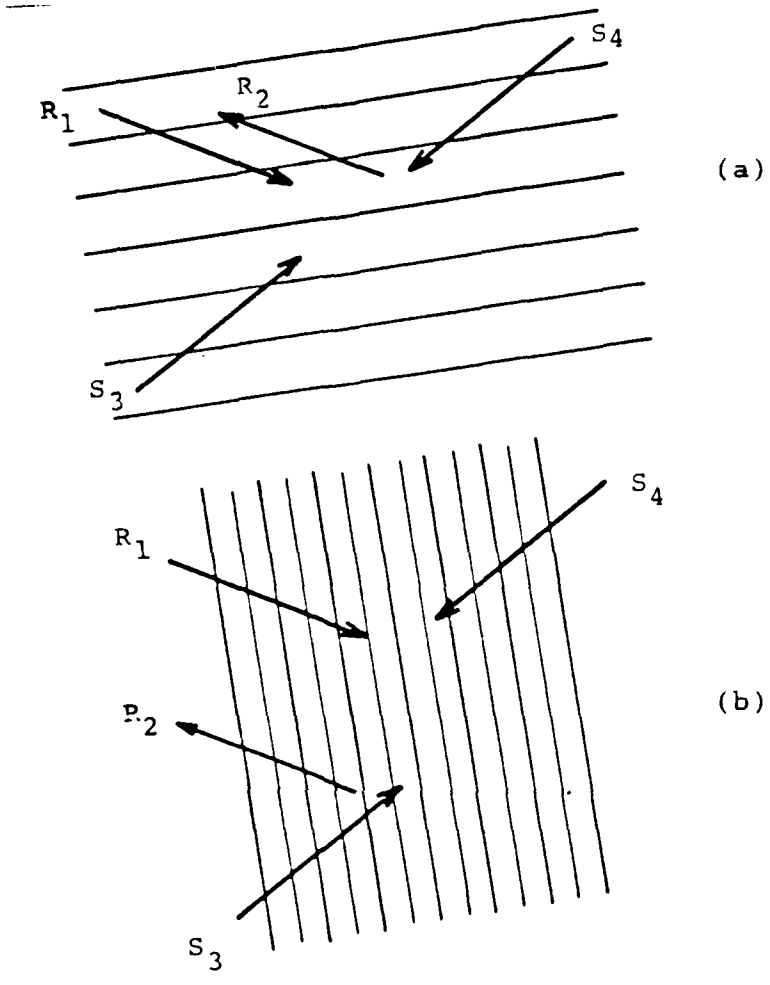

Figure 8. (a) Grating formed by R_1 and S_3 (b) Grating formed by R_2 and S_3 [Ref. 2: p. 50]

FWM can be used even if the signal beam differs from the reference beams by a small amount in frequency [Ref. 3: p. 51]. The gratings would then move with a small constant velocity, and the necessary frequency shift to produce the phase conjugate beam can be seen as a Doppler shift from a moving grating.

It is also possible to get a reflectivity of the PCM in excess of unity [Ref. 4: p. 257]. This depends on the value of the electro-optic tensor for the material used, and is highly sensitive to the relative intensities of the three beams and their orientation. Reflectivity values as high as 30 have been obtained with $BaTiO_3$ [Ref. 12: p. 362].

If the crystal is sufficiently responsive, a number of variations of four wave mixing for generation of phase conjugate waves are possible. For a material that exhibits gain, inputting just the two reference beams and placing a mirror where the signal beam usually is, creates a cavity that self-oscillates. S_3 and S_4 are generated by diffraction of light within the crystal which is reflected back by the mirror and creates the usual gratings with the reference beams. The signal beam which does not reflect off the mirror can be used as the output beam, and through two beam coupling with the reference beams the output power can be greater than the power oscillating in the cavity.

Another variation on FWM used to generate phase conjugate waves is known as self-pumping. In this set up, only the signal beam to be conjugated enters the crystal, the others are generated internally. The beam enters the crystal at an angle with the c axis. Asymmetric self-defocusing produces a fan of light in the plane of the beam and the c axis due to the photorefractive effect [Ref. 13: p. 486]. Some of the rays of the fan undergo internal

reflection by a corner of the crystal twice and return towards the incident beam. Each ray has a corresponding counterpropagating ray which separated from the incident beam where the former ray returns. (see Figure 9) The counterpropagating rays form the reference beams generating the phase conjugate wave.

Each interaction region is described by four coupled wave equations. The solution to these [Ref. 13: p. 487] predicts that self-pumping will turn on when $\beta l >= 2.34$, where l is the effective length of each interaction region, and β is the coupling constant per unit length given by

$$\beta = (w/2nc)\{E_{eff}/\cos((\alpha_1 - \alpha_2/2))\}. \quad (17)$$

α_1 and α_2 are the angles of the rays with the c axis, w is the optical frequency, n is the index of refraction, E is the electric field, and r_{eff} is the Pockels coefficient. If there is no applied electric field, E is given by

$$E = (k_B T/q)\{k/(1+(k/k_o)^2), \quad (18)$$

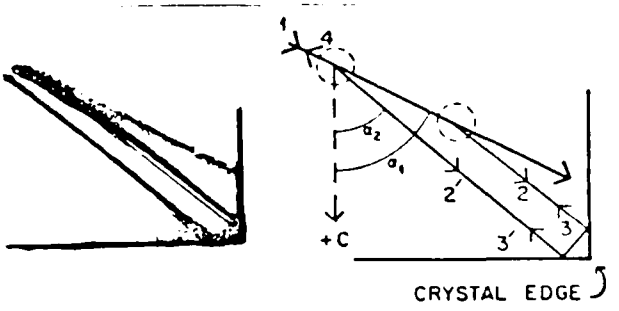

Figure 9. Beam Geometry For Self-pumping 1)Incident beam 2')Ray initially diffracted 2)Ray diffracted where ray 3 returns 3)Ray 2' after reflection 3')Ray 2 after reflection [Ref. 13: p. 487]

where q is the charge of the carrier, $k_B T$ is the thermal energy, k is the magnitude of the wave vector, and k_o is a parameter determined by the charge density. In this geometry

$$k = 2(nw/c)\sin[(\alpha_1 - \alpha_2)/2], \tag{19}$$

and

$$k_o = (Nq^2/(\epsilon\epsilon_o k_B T))^{1/2}, \tag{20}$$

where N is the number density of charges available for migration, and $\epsilon\epsilon_o$ is the static dielectric constant in the direction of **k**.

As an example of why the polarization of the incident beam is so important, for crystals of a symmetry similar to $BaTiO_3$, r_{eff} for ordinary rays is given by

$$r_{eff} = n_o^4 r_{13} \sin((\alpha_1 + \alpha_2)/2), \tag{21}$$

and for extraordinary rays is given by

$$\begin{aligned} r_{eff} = \sin((\alpha_1 + \alpha_2)/2) \{ & n_o^4 r_{13} \cos\alpha_1 \cos\alpha_2 + \\ & 2 n_e^2 n_o^2 r_{42} \cos^2((\alpha_1 + \alpha_2)/2) + \\ & n_e^4 r_{33} \sin\alpha_1 \sin\alpha_2 \}. \end{aligned} \tag{22}$$

Since r_{42}, the electro-optic tensor component, is generally larger than the other terms, the use of extraordinary rays greatly enhances the onset of self-pumping.

E. HOLOGRAPHIC ANALOGY

A hologram is an interference pattern made with coherent light beams, stored in a medium such as photographic film. Coherent light from an object beam and a reference beam forms the interference pattern. The image of the object is

recreated by exposing the hologram to a coherent source. The geometry of the reference and subject beams in FWM grating formation is similar to that of the reference and object beams in holography. Because the phase gratings persist in the photorefractive material until washed out by the dark current, the gratings are often referred to as volume phase holograms.

The phase gratings can be thought of as the three dimensional equivalent of holograms. Through the phase conjugate properties, images can be stored and read out even if there are distortions in the writing/reading beams [Ref. 13: p. 487].

Although there is a close analogy between holography and this form of phase conjugation, there are important differences. The first is that conventional holograms must be developed before they can be read out. Phase conjugation occurs on a real time basis, and can adapt to changes in the object beam, whether due to changes in the beam itself or along the path of propagation. Second, holograms modify some gross physical feature of the recording medium in a semipermanent way. If the object and reference beams are not of the same frequency, a moving interference pattern will form, washing out the hologram. This does not happen in phase conjugation.

F. PHASE CONJUGATION IN $BaTiO_3$

Barium titanate is classified as an oxygen-octrahedra ferroelectric photoconductive crystal [Ref. 4]. It has a tetragonal structure at room temperature, and undergoes a phase transition to orthorhombic at 5° C and a phase transition to cubic at between 128 and 133° C. The photorefractive efficiency of the crystal depends on the dopants introduced during crystal growth. Iron seems to give the greatest sensitivity. The difference in the valence between the Fe and the normal balance of Ba and Ti in the lattice is compensated by oxygen vacancies in a roughly octrahedral array around the substitution site [Ref. 4: p. 233]. Each crystal will have a slightly different composition, so the physical properties, including phase transition temperature will vary. One limit on the applications of these crystals is their size, which is limited by the ability to grow large crystals of a single domain. The present limit is about 1-2 cm^3 [Ref. 4:p.236].

The index of refraction of barium titanate is 2.488 for ordinary rays, and 2.424 for extraordinary rays at 515 nm. The dielectric constants at room temperature are 168 parallel to the c axis and 4300 perpendicular to it. The nonzero elements of the electro-optic tensor are approximately 80 pm/V for r_{13} and r_{33}, and 1640 pm/V for $r_{42} = r_{51}$. The dark conductivity is $1.3X10^{-12}$ $(ohm\ cm)^{-1}$. [Ref.

4: pp. 214,223] This gives a storage time of only 15 hours for this material.

The large value of the r_{42} component makes use of the extraordinary ray important if phase conjugation is to be observed. Lasers need to be polarized in the plane formed by the incident beam and the c axis.

With no external applied electric field, the primary means of charge migration in barium titanate are diffusion and drift. The photovoltaic field E_{ph} is <300 V/cm [Ref. 8: p. 818]. Beam coupling experiments by Feinberg [Ref. 7] have shown that the sign of the charge carrier is positive. The mean charge migration length per optical excitation is

$$L_m = n_{ph} h\nu / e, \tag{23}$$

where n_{ph} is the photoconductive constant, and ν the frequency. Measured values for n_{ph} are about 10^{-9} cm/V [Ref. 8: p. 818]. Diffusion and drift lengths are 0.2 and 0.7 microns respectively, while the photovoltaic migration length is 0.76 angstroms [Ref. 4: p. 239].

The rate at which a grating is written by a light pattern is the same as the rate at which it is erased by the light, so if the dark current is included

$$R = R_d + R_l, \tag{24}$$

where R_d is the dark erasure rate and R_l the light erasure rate.

$$R_d \propto (1 + k^2/k_o^2) \exp(-T/T_o), \tag{25}$$

and

$$R_1 \propto (1 + k^2/k_o^2)\,(I/I_o)^x, \qquad (26)$$

where T is the crystal temperature, I is the erasure intensity, I_o is $1 W/cm^2$, and T_o and x are determined by experiment. The other terms are as previously defined.[Ref. 9: p. 2]

Values for the intensity dependence were measured by Ducharme [Ref. 9] and range from x = 0.62 at 16° C to 0.71 at 40° C. Measurements were also made of the temperature reference value T_o. Depending on the crystal used, T_o = 11800 +/-400° K to 8000° K. [Ref. 9] These results indicate a strong temperature dependence for the grating erasure rate, so elevated temperatures will reduce the storage time and make the grating more difficult to write.

Applying an external electric field to the barium titanate crystal increases the force on the moving charge carriers, increasing the mean displacement per optical excitation. With no field applied, the force on the charges was shown to be proportional to the wave vector **k** (Equation 18), whereas with an applied field the force can be made almost independent of **k** by choosing the proper value for E_{ex}. This external field is applied in the direction of the c axis so that the effects contribute to the refractive index changes induced without an applied field. The refractive index increases almost linearly with applied field above 2 kV/cm, reaching a maximum change of a factor of five at around 10 kV/cm with no degradation in optical

quality. If E_{ex} is applied in the direction opposite to the c axis, beam distortion and stray light arise due to depoling effects for E_{ex} > 1 kV/cm.[Ref. 8: p. 818]

Measurements of the response of barium titanate to increasing wavelength show that an increasing amount of optical energy is required for phase conjugation. This can be either an increase in intensity or time (up to the limit of the dark current for that crystal). At 515 nm, an energy of 0.04J/cm^2 (0.4 seconds) is required for a 0.1 W/cm^2 beam [Ref. 14: p. 476]. This increases to 18 J/cm^2 at 0.80 μm (120 seconds using a 3 mW beam focused to 150 mW/cm^2), and to 600 J/cm^2 at 1.06 μm (10 minutes using a 35 mW beam focused to 1 W/cm^2) [Ref. 10: p. 627]. This is the time required to set up the grating, but once established the response to small changes in the input signal will occur much more rapidly. The response to very high intensities has been tested at 532 nm. Using 20 nanosecond pulses, the energy needed to establish a grating is 0.45 J/cm^2, but this requires an intensity of 5 to 30 MW/cm^2 [Ref. 14: p. 476]. To establish self-pumping with a continuous wave laser, a power level of 0.8 mW/cm^2 is required if the crystal is in the dark, and 4.0 mW/cm^2 if it is in ambient light [Ref. 12: p. 364]. The higher power required in ambient light is to overcome the even redistribution of charges caused by the uniform illumination.

Besides four wave mixing, barium titanate can be used to generate phase conjugate waves by several other methods. The longer wavelengths (i.e., 1.06 μm) require a ring cavity arrangement in which the incoming beam wave vector is parallel or antiparallel to the c axis [Ref. 10]. Stimulated backscattering, in an arrangement much like stimulated Brillouin scattering has also been used [Ref. 15].

III. EXPERIMENTAL INVESTIGATION

A. OVERVIEW

The objective of these experiments was to demonstrate optical phase conjugation in barium titanate, and identify those parameters that affect the speed and performance of phase conjugation in this crystal. Using the equipment available, the parameters which could be varied included the power and intensity of the incident beam, and the angle between the incident beam and the c axis of the crystal. Based on these results, a determination could be made as to whether $BaTiO_3$ should be a candidate for attempts to correct distortion of a laser beam propagated over a distance.

B. $BaTiO_3$ POLING EXPERIMENTS

$BaTiO_3$ at room temperature is a yellow-tinged crystal. The coloring comes from the crystal impurities. The crystal is fairly soft, being easily scratched, and will fracture if dropped. Handling must be done with soft plastic tweezers. Teflon tweezers will scratch the crystal. The crystal temperature must also be controlled. Approaching the phase transition temperature at 6° C can cause the crystal to crack, and heating the crystal for prolonged periods near the phase transition at around 130° C can depole it. Excessive heatup and cooldown rates can also damage the crystal. Methanol can be used to clean the crystal.

Acetone may be used, but cracking can occur from the fast cooldown rate produced by evaporation of the acetone.

The $BaTiO_3$ crystal obtained from Sanders Associates measured 0.5 X 0.5 X 0.5 cm. It had been mechanically pulled, but no electric field had been applied for poling the ferroelectric domains.

The c axis was determined by using crossed polarizers. Two standard pieces of linear polarizing material were aligned with their axes at 90 degrees for extinction and the crystal placed between them. When viewed through the polarizers, the crystal will go from light to dark and back as it is rotated around the viewing axis for the two directions perpendicular to the c axis. When viewed through the c axis, the crystal will not lighten and darken when rotated, and will appear multicolored, much like a thin film interference pattern.

To determine if the crystal was sufficiently poled, it was tested for two beam coupling using the setup described above. The source was a Spectra Physics Model 162 15 mW Ar-ion laser set to the 514 nm line. A rhombic prism was used to split the beam, and beam intersection angles from 15 to 25 degrees were tested. After one minute there was no change in power level for either beam, and no change from the power level measured when the beams passed through the crystal but did not intersect. All six crystal orientations were tested and no evidence of poling was detected.

The method for poling the crystal varies slightly depending on the degree of risk and success desired. The procedure used here has been used successfully by Feinberg [Ref. 6: p. 286]. Some crystals can not be poled. These have an improper balance of oxygen vacancies and iron impurities [Ref. 6: p. 283]. The telltale indication is a transition temperature near 125° C instead of elsewhere in the range of 120 to 133° C.

The poling procedure is as follows: Apply two electrodes which are larger than the face of the crystal in such a direction that the electric field applied will be in the direction of the c axis. If partial poling of the crystal was observed during two beam coupling, the field should be applied in the direction of coupling. The electrodes should not be made of a material which will diffuse into the crystal during poling such as silver or gold. Chrome plated brass works best [Ref 6: p. 286]. Polishing the surfaces which touch the crystal reduces damage to the crystal faces. The crystal can be suspended between the electrodes by using moderate spring pressure.

The crystal and electrodes are placed in a cuvette filled with Dow Corning 200 fluid (A Dimethyl-polysiloxane) of a sufficiently low viscosity to allow thermal mixing e.g. 50 or 100 cs. This was chosen because it had a breakdown voltage of 16000 V/mm. Suspend the cuvette in a mineral oil bath (0.8 to 1.5 l) on a hot plate. Allow about

1.5 cm in the beaker for thermal expansion of the oil. The cuvette should be supported on an insulator so that it does not touch the hot surface. The assembly needs to be shielded from air currents.

Slowly heat the crystal to the phase transition point. The heatup rate should not exceed 20 deg/hour below 100° C., 5 deg/hr between 100 and 120° C., and 2 deg/hr above 120° C. Monitor the temperature carefully with an accurate thermometer. The oil must be mixed to maintain a uniform temperature. Gentle stirring every few minutes is sufficient. Measure the capacitance across the crystal as a function of temperature. If the capacitance has not increased significantly (only 10 pf or so) by 120° C., the electrodes may not be properly seated against the crystal. Apply 1000 V in steps of 100 V every 10 to 15 sec., then reduce and remove the voltage and continue the heatup. The capacitance should have jumped to the proper value.

There are several indications of the transition point. The capacitance will increase sharply from an initial value of around 30 pf to a value of 50 to 100 pf. Well beyond the transition point the capacitance will decrease. The best indication is to observe the birefringence of the crystal. This may be observed by placing crossed polarizers on either side of the oil beaker with a strong light on the other side. The crystal can only be viewed perpendicular to the c axis since the electrodes block the direction parallel to

the c axis. Striking colors will appear at the transition point. Occasionally domain walls can be seen in the crystal, either at room temperature, or as the crystal is heated. The walls appear as diagonal lines. They will disappear at the transition point.

As soon as the transition point is reached, apply a DC electric field of 1250 V (actually about 250 V per millimeter of crystal). The field should be applied in step increments over one to two minutes. Commence cooldown as soon as the field is applied to minimize time spent near the transition temperature. The cooldown rate used above 120° C should be twice that used during the heatup, while the same rate can be used below that temperature. Once the cooldown is complete, remove the electric field in increments just as it was applied. Clean the crystal to remove residual oil.

The crystal may take on a muddy appearance at the transition temperature, or domain walls may appear during the initial stages of cooldown. Both of these should disappear as the cooldown progresses. Some damage may occur to the crystal at the positive electrode face. This can consist of minor surface cracks or scratches, or even blackening of the crystal face. These will not interfere with the operation of the crystal. If desired they may be removed by polishing using an optical flat. To reduce the time required for the experimenter to spend without a break, the crystal may be heated to about 60° C then left

overnight. During cooldown the crystal may also be left overnight between 60 and 80° C.

An alternative procedure, used by Sanders Associates, is to heat the crystal only to 125° C, then apply an electric field of 1000 V for one hour. The crystal is then cooled down with the field still applied. The field is applied for longer at the higher temperature because it takes more energy to break down the domain walls further away from the transition temperature. This procedure is more conservative in approach, and may not guarantee complete poling. However, either procedure may be repeated as necessary.

Equipment necessary to pole the crystal was assembled and tested, and several trial runs made to practice control of the heatup and cooldown rate. This was found to be much more difficult than previously thought and required constant monitoring. For this reason the actual run was done without leaving the crystal overnight.

A graph of capacitance as a function of temperature is included as Figure 10. The capacitance measured was that for the crystal and electrode assembly rather than just the crystal and therefore starts at 143.2 pf rather than around 30 pf. At 120° C, 1225 V was applied and removed. The heatup was continued but the expected indications of the transition point were not observed. At 133° C a diagonal discontinuity was observed to move across the crystal and disappear. Since this was the maximum temperature to which

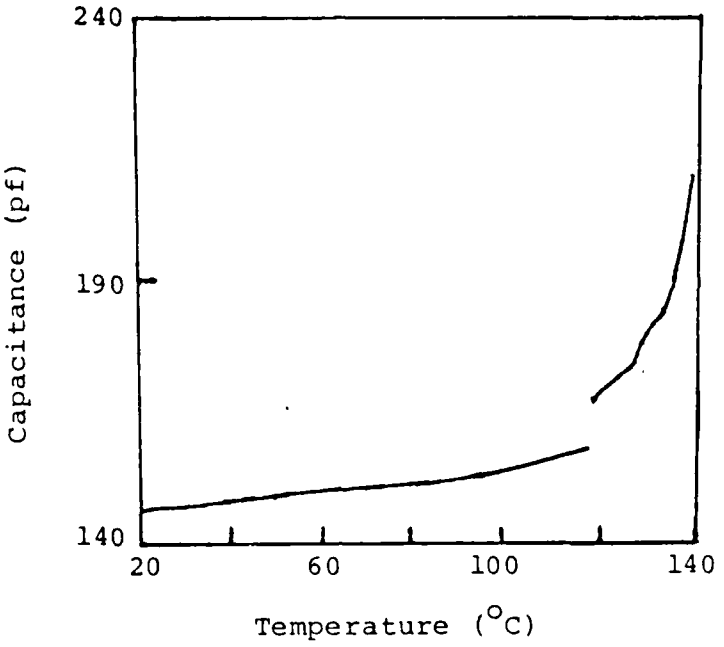

Figure 10. Capacitance as a Function of Time During Heatup (Discontinuity is due to applying DC voltage across crystal)

the heatup had been planned, and corresponded to the high end of the transition temperature range, it was decided that this must be the phase transition moving through the crystal. The electric field was applied and cooldown commenced immediately. Between 130 and 128° C a diamond shaped opaque plane appeared in the crystal parallel to the c axis. The diamond remained in the crystal after cooldown had been completed. Testing of the crystal determined that a laser beam would not propagate through the crystal in any direction without extensive reflections and dispersion. The diamond appeared to be an internal crack between two crystal

planes bounded by domain walls. Since this crystal proved useless, a new crystal was placed on order. The delivery time by Sanders Associates is about six months. Crystals take several months to grow, and then are cut and polished at a rate of about one a week. Of these, only about 30% prove usable for phase conjugation.

C. HOLOGRAPHIC EXPERIMENTS

As discussed in Section II, there is a close analogy between holography and phase conjugation. While waiting for delivery of a second barium titanate crystal, a Newport HC-300 Holographic Recording Device was tested with a view toward using it to measure distortions imposed on a laser beam during propagation.

This machine uses a thermoplastic film as the exposure medium. The recording plate is a two layer material, consisting of a thin thermoplastic over a photoconductor. This is supported by a transparent silica substrate. To construct a hologram, the plate is first given a uniform surface electric charge, then exposed to the laser interference pattern caused by a reference beam and light reflected from the object. Those parts of the film exposed to the light portions of the pattern have their charge transported through the photoconductor toward the thermoplastic film. The plate is then given another uniform surface charge and heated. Those areas of the plate previously exposed to light will now have more electric

charge, and upon heating, electrostatic attraction will squeeze the thermoplastic film thinner than dark areas. This creates a phase grating that will diffract light to reconstruct the original pattern. Erasure is performed by controlled, uniform heating of the plate.

The advantages of this method are that it takes the about one minute to expose and develope a hologram, and that the diffraction efficiency is 10 to 30 times higher than conventional holography. A standard holographic exposure set up was used (see Figure 11) with a 15 mW Argon ion laser set to 488 nm as the source. The path lengths for the

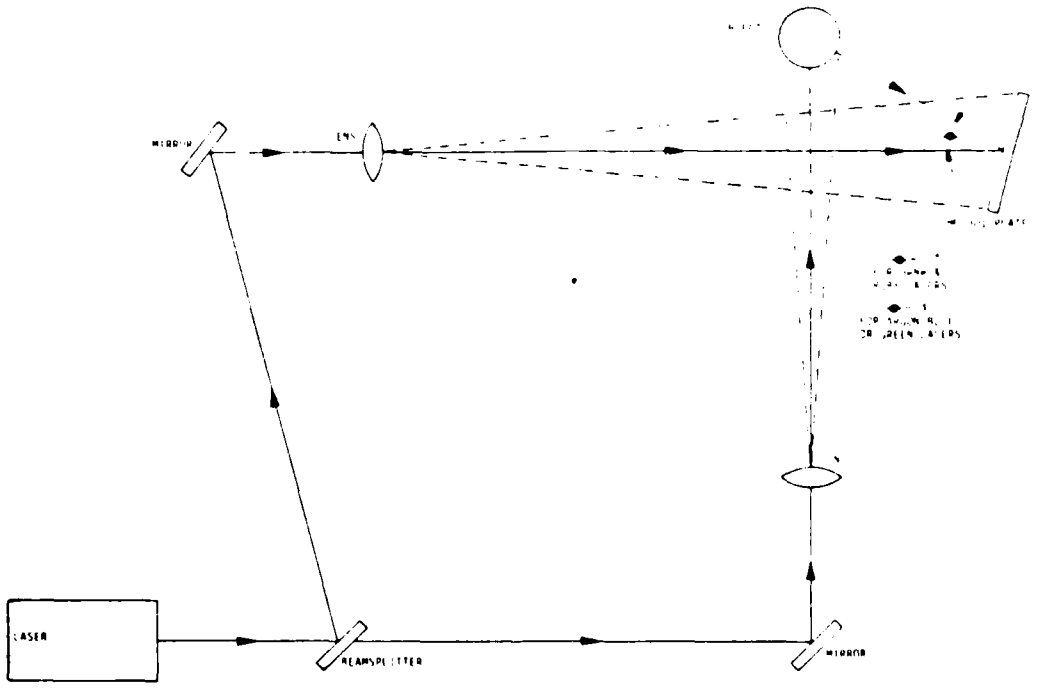

Figure 11. Optical Arrangement For Producing Holograms (Diagram from HC-300 Operating Manual)

reference and object beams were the same to within 0.5 cm, and the angle between the reference beam and the object beam at the film was set at the optimum recommended angle for this wavelength of 25°.

The hologram machine automatically developed the film for the correct amount of time depending on the measured exposure. Exposure times ranging from a half to thirty seconds were tested. All of the exposures were completely blurred. The cause was vibrations in the laser beam caused by the laser cooling fan. The fan in this model laser is hard mounted to the laser cavity assembly, producing vibrations that can be felt on the laser body and, through the mounts, on other equipment along the optic bench. This observation proved to be an important factor later in trying to produce conjugate waves in barium titanate.

A 1.0 mW HeNe laser produced good exposures consistently, even though the power level of the reference beam was only 0.05 mW at the film. Exposure times of from 0.5 to 2.0 seconds produced the sharpest images, with some degradation in image quality occurring for times longer than 10 seconds.

The procedure for observing distortions in the path length for the laser beam was to make an exposure of an object, then without moving the object, re-illuminate and view the object through the holographic film. Light from the object would form an interference pattern with the

image. Dark lines, much like a thin film interference pattern, could be seen. As an indication of the sensitivity, the residual heat from a momentary fingerprint would displace the object sufficiently for fringes to form, and they could be seen to shrink as the object cooled. Rapidly shifting fringes due to turbulence along the path of propagation caused by a candle, or even a hand held beneath the beam, could also be seen. Figure 12a shows the holographic image of a flat aluminum plate before introducing distortions. Figure 12b shows the same image after a small thermal distortion.

Further experiments such as setting up a high speed counter for measuring changes from the standard path length through fringe counting were not conducted because another barium titanate crystal became available at this time.

D. $BaTiO_3$ PHASE CONJUGATION EXPERIMENTS

A second barium titanate crystal was obtained on loan from Harry Diamond Laboratory. The crystal measured 0.3 X 0.3 X 0.3 cm, and had been used to produce self-pumped phase conjugate waves from an input beam in the hundred milliwatt range.

The crystal was set up in the standard self-pumping set up described previously. A Spectra Physics Model 162 15 mW Argon ion laser was used as the source, and a microscope slide used as the beamsplitter. The laser produces light of vertical polarization, and attempts to produce a phase

(a)

(b)

Figure 12. (a)Holographic Image of a Flat Plate
(b)Interference Pattern Due to Optical Path Distortion

conjugate return were unsuccessful. Initially, a return beam was detected which appeared to exhibit some phase conjugate properties. The beam reflected off the beamsplitter on its return from the crystal, and was smaller and sharper than the return off a mirror substituted for the crystal. However, although the beam did not move when the crystal was rotated horizontally, it did move when the crystal was moved vertically. In addition, the beam that passed through the beamsplitter did not enter the laser cavity, but struck the housing about a centimeter away. Since the return appeared immediately upon illumination of the crystal, and only appeared when the incident beam made a 45° angle with the c axis, the return was determined to be a double internal reflection off the back corner of the crystal.

The laser vibrations caused by the cooling fan, which had earlier prevented the laser from being usable for holography, were thought to be a major reason for the inability to obtain a phase conjugate return. A 5 mW HeNe laser was obtained, and attempts were made with the laser standing upright (which produced vertical polarization), and with the laser lying on its side. No return was detected. It was discovered in a subsequent phone conversation with Mary Tobin of Harry Diamond Laboratory, that it was extremely difficult to obtain phase conjugation in the red wavelengths, often requiring 20 minutes or more at 100 mW.

The Argon ion laser was laid on its side to produce horizontal polarization, and isolated from the optical table using bubble insulation to reduce vibration. A phase conjugate return was obtained which measured 0.04 mW, just at the low end of the detector's operating range. This corresponded to an approximate phase conjugate return of 20%. The return was clearly identified as a phase conjugate beam, because it did not exhibit any of the anomalies earlier identified with the back corner reflections, and because distortions placed along the path of propagation (such as a piece of glass) did not affect the return other than to reduce its intensity. The conjugate beam appeared as two small spots due to reflection off the front and back faces of the beamsplitter. This was identical to the incident beam reflection off the other side of the beamsplitter.

The appearance of the beams inside the crystal was virtually the same as that shown in Figure 9. When the crystal was illuminated in a configuration that would not allow phase conjugation, the incident beam could be seen (by scattering) refracting in the normal way upon entering and leaving the crystal. In a phase conjugate configuration, the incident beam smeared out upon entering the crystal so that it could no longer be seen. After a few seconds the crystal started to fluoresce, and scattering from the corners became noticeable. As conjugation began, a ray

arcing towards the back corner became evident, and sometimes could be discerned as two distinct parts. The arcing ray would seek out the back corner despite any changes in the incident angle. The portion of the incident beam not scattered or internally reflected, was transmitted through the crystal after undergoing the usual refraction.

The initial phase conjugate beam visibly vibrated on the detector, and would not start consistently. Measurements made were not reproducible. This was blamed on laser vibrations, and on laser beam instabilities caused by a fault in the laser power supply which interrupted the beam every few minutes.

A new power supply for the laser corrected the beam interrupt problem, and a Babinet compensator with a quarter wave plate made for the green line of mercury converted 95% of the laser beam to horizontal polarization. This allowed the laser to remain upright, but introduced a 32% loss in intensity of the beam. The cooling fan was mechanically decoupled from the laser body by removing the screws which penetrated the insulation, and bubble insulation was placed under the laser supports. This reduced the vibrations to below the level at which they could be felt on other components along the optic bench. Because the beamsplitter was only reflecting 2% of the incident light (due to operation near Brewster's angle), the detector was replaced with a more sensitive Si semiconductor detector. This

equipment greatly improved the quality and reproducibility of the data.

The first set of measurements taken were to determine the magnitude of the conjugate return, and whether the values varied with power level. The Argon ion laser was set to its optimum output line of 488 nm, and the crystal oriented so the incident beam made a 45° angle with the c axis. This angle was chosen based on information received with the crystal that this direction worked well for this crystal. The laser output power was varied from 1.0 to 10.0 mW.

The power of the phase conjugate beam return followed an S shaped curve. A typical output from the detector is shown in Figure 13. The final amount of phase conjugate return was independent of the laser power, and the average return was 28.2% of the power entering the crystal. Including all subsequent measurements made at 488 nm and an incident angle of 45°, the overall average was 25.3%. Each phase conjugate return varied with time between 4 and 8% of its mean value. The amount of variation depended on the power of the incident beam.

To determine if the variations were due to feedback of the conjugate beam into the laser, the laser output reflected off the beamsplitter was measured in both constant current control mode and constant optical power control mode. The results with the beam into the crystal blocked

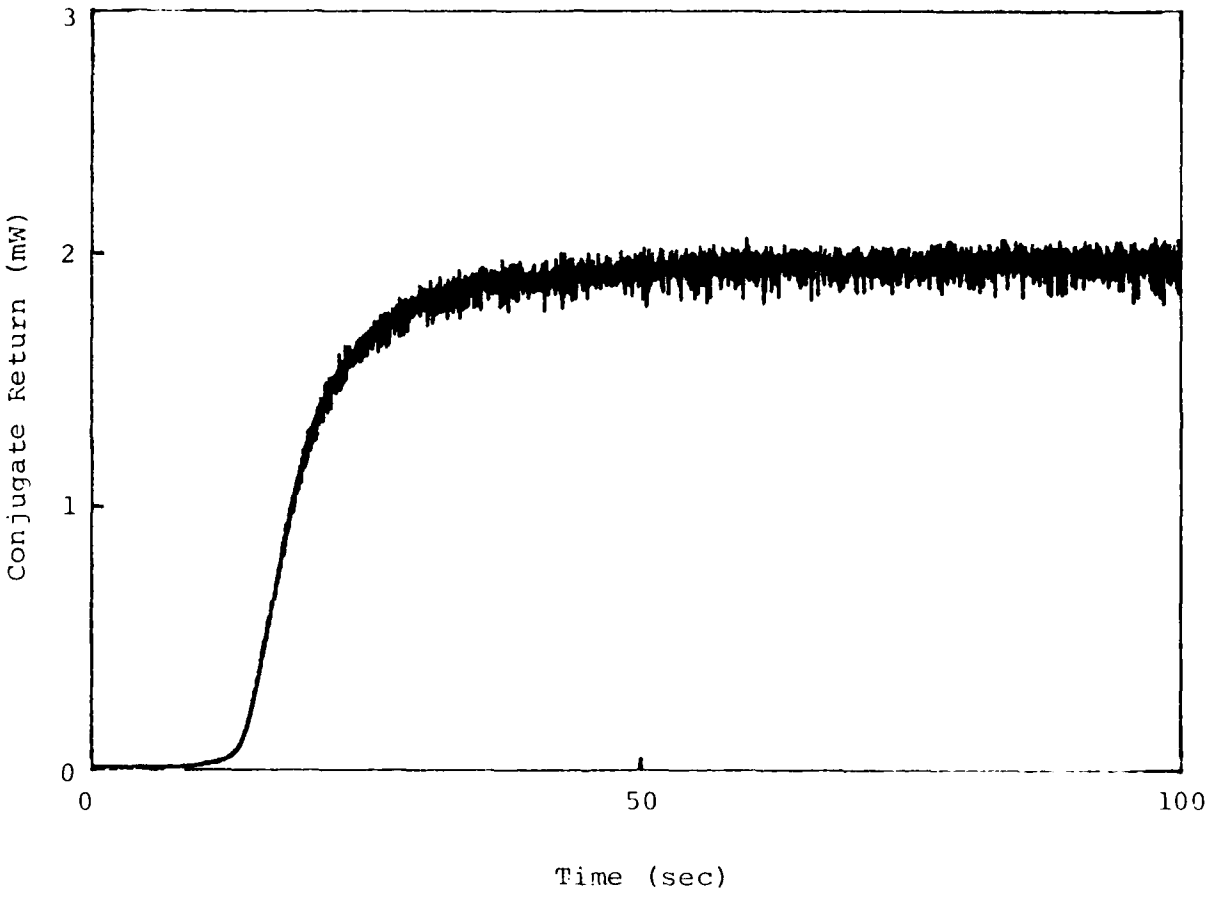

Figure 13. Conjugate Return for 488 nm, 8 mW Incident Power

off were compared to the results with conjugate feedback. The conjugate beam strongly affected the standing modes inside the laser cavity for both laser power supply control modes. This occurred despite the 32% loss experienced each time the beam traveled through the Babinet compensator and quarter wave plate. This effect is shown in Figures 14 and 15.

The next set of measurements were of the time the phase grating remained in the crystal at a usable level. A grating was established in the crystal by waiting for a strong phase conjugate return, then the incident beam was interrupted for increasing amounts of time. The time taken for the conjugate beam to return to its original level was then measured. For comparison, the time required for a response to a small displacement of the crystal was measured by rapidly rotating the crystal a few degrees until the conjugate return disappeared. Interrupts were performed with the room lights off to measure the dark conductivity of the crystal.

For interrupt times less than two minutes, the conjugate response began immediately, and built to its final value. For interrupt times of two minutes or more, the build up followed an S shaped curve, but the onset of the response required an increasing amount of time for increasing interrupt times. The response time as a function of interrupt time increased exponentially, as is shown in

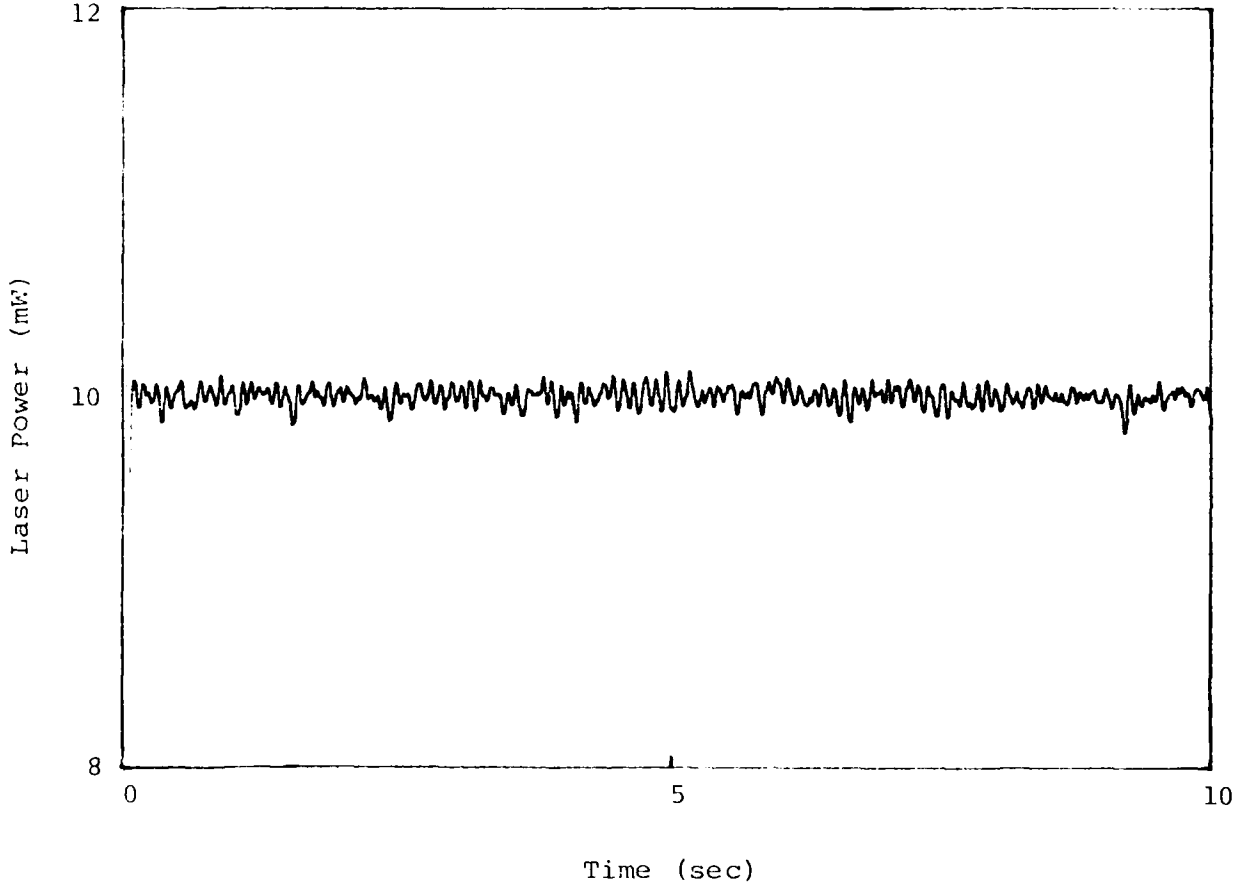

Figure 14. Laser Power With Conjugate Feedback

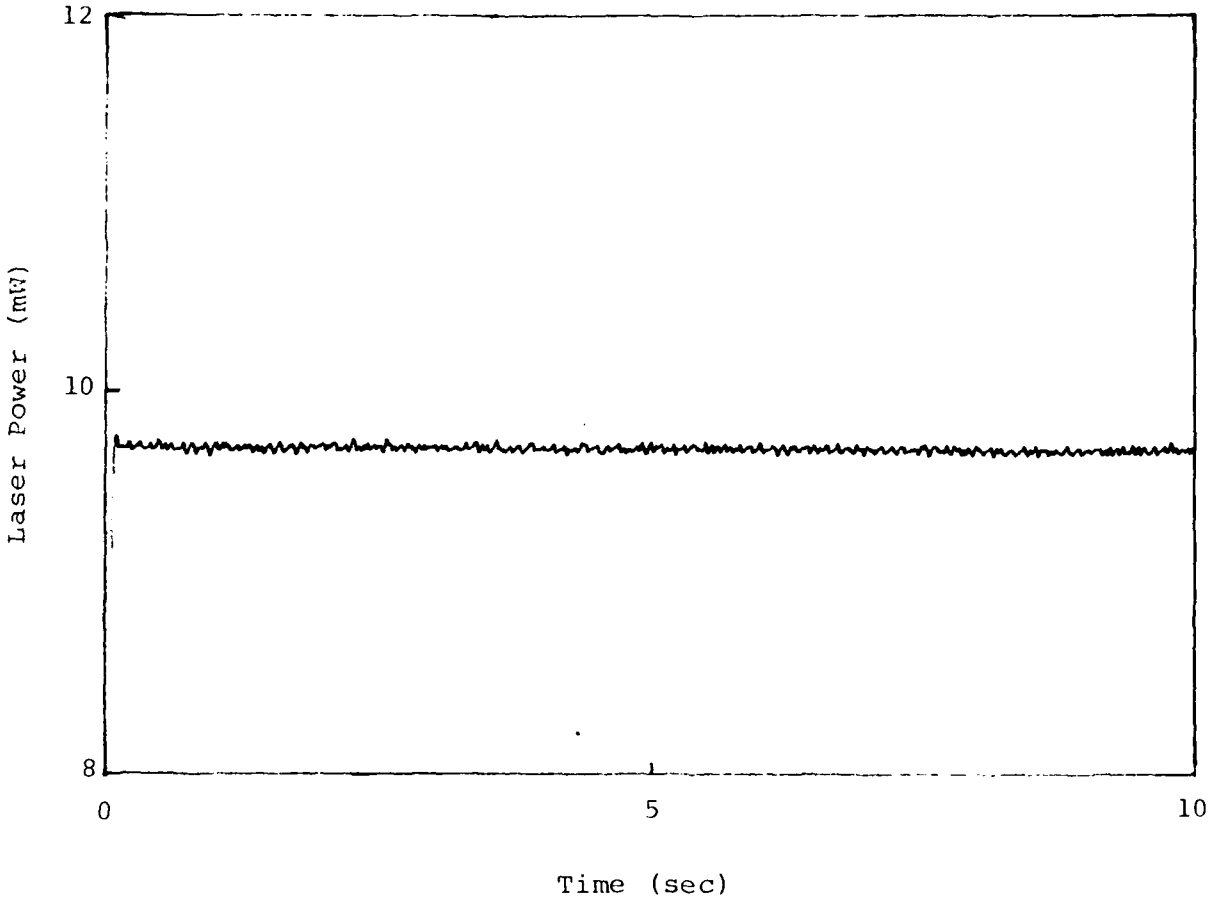

Figure 15. Laser Power Without Conjugate Feedback

Figure 16. Moving the crystal by a few degrees corresponded to interrupting the beam for two to four minutes. These results indicated that a significant portion of the grating remained in the crystal for several minutes. When the grating decayed below a certain minimum threshold, it had to be built up again before phase conjugation would start. Some of the charges that make up the grating remained in

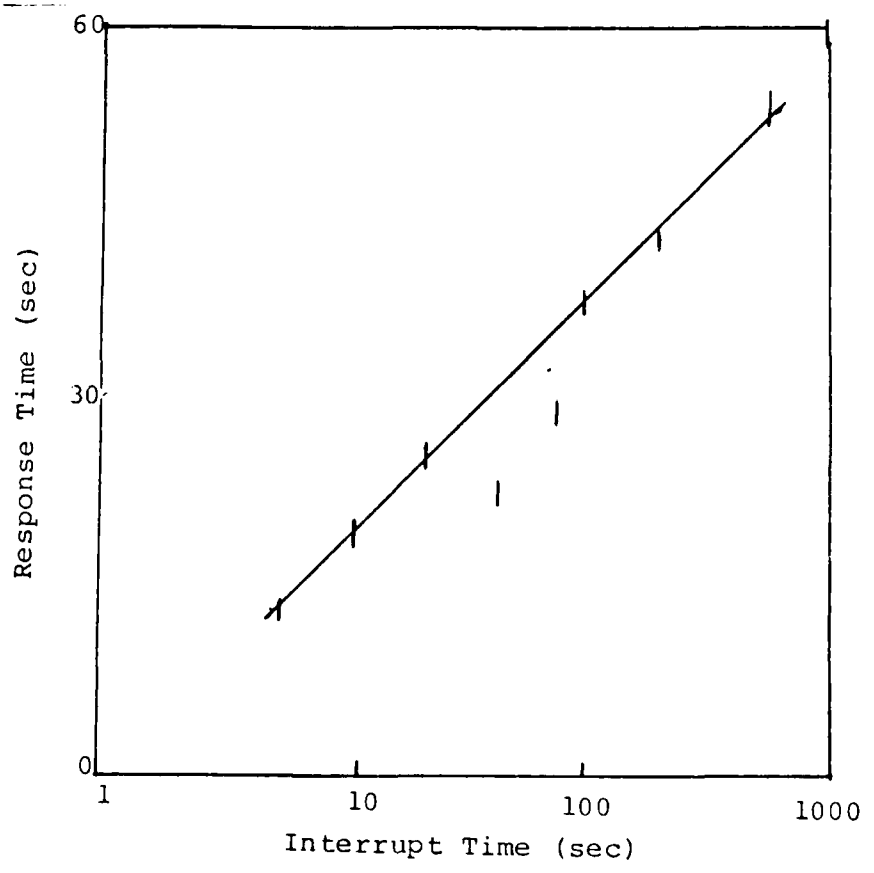

Figure 16 Response Time of the Conjugate Beam as a Function of Interrupt Time for 488 nm, 4 mW Incident Power

place for up to ten minutes, and these only needed to be added to, or in the case of a small displacement rearranged slightly, to produce a response.

The results for the ten minute interruption corresponded closely to those obtained just prior to this set of measurements using the identical laser power setting and crystal placement. In this case the crystal had been unexposed since the previous day. This indicated that the grating decayed away completely in ten minutes. To ensure that response times would not be influenced by previous exposures, all subsequent measurements were made with a ten minute wait between them.

The next set of measurements taken determined the phase conjugate response of the crystal as a function of angle between the incident beam and the c axis. The laser was set to 488 nm and a constant power level, and the time to initial response and the amount of final response were recorded in five degree increments. The energy needed to start phase conjugation, and the amount of phase conjugation as a function of angle, are summarized in Figure 17. Data for angles less than 20° were not accurate because the diameter of the incident beam was then larger than the cross section of the face of the crystal. At 15° the initial response took more than five minutes, and peaked after 35 minutes. A significant portion of the beam was being transmitted through the crystal, and a new reflected beam

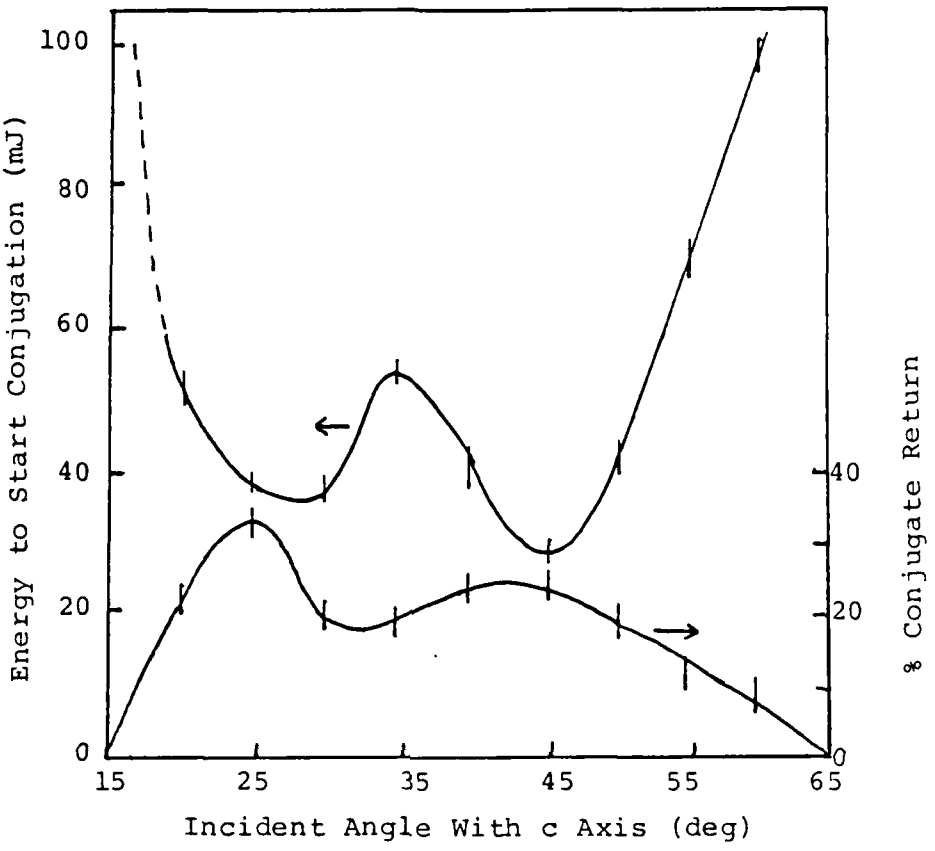

Figure 17. Energy to Start Conjugation, and Percent Conjugate Return as a Function of Incident Angle for 488 nm, 6 mW Incident Power

appeared returning on the opposite side of the c axis at an angle of about 20°. The rays shown in Figure 9 were not visible except as a bright smeared out area near the back end of the crystal. At 65° no phase conjugate response was obtained. Fluorescence did not occur, and the incident beam propagated through the crystal with normal refraction.

The maximum response occurred for angles of 45° and 25°. By calculating energy and percent conjugation, changes in response due to differences in the laser power could be eliminated. The reason for the decrease in response around 35° is not known. The index of refraction for the extraordinary ray in barium titanate is 2.42, which makes Brewster's angle 22°. To verify the amount of incident beam being transmitted into the crystal, the power of the beam reflected from the face of the crystal was also measured as a function of angle. The data supports an index of refraction of greater than 2.2. This value was again limited by the cross sectional area of the crystal at small angles. Correction for the power actually entering the crystal did not significantly change the shape of the response curves, and the corrected curve is shown in Figure 17.

The final set of measurements taken were to determine the amount of energy required to establish a phase conjugate grating as a function of incident power and frequency. The laser was tuned in turn to each of the six visible lines obtainable from this Argon ion laser, and the response recorded for several values of power over the range available. These results are shown in Figures 18 and 19 and 20.

The values of energy required for 488 nm were lower than expected in many cases, and did not show any regular

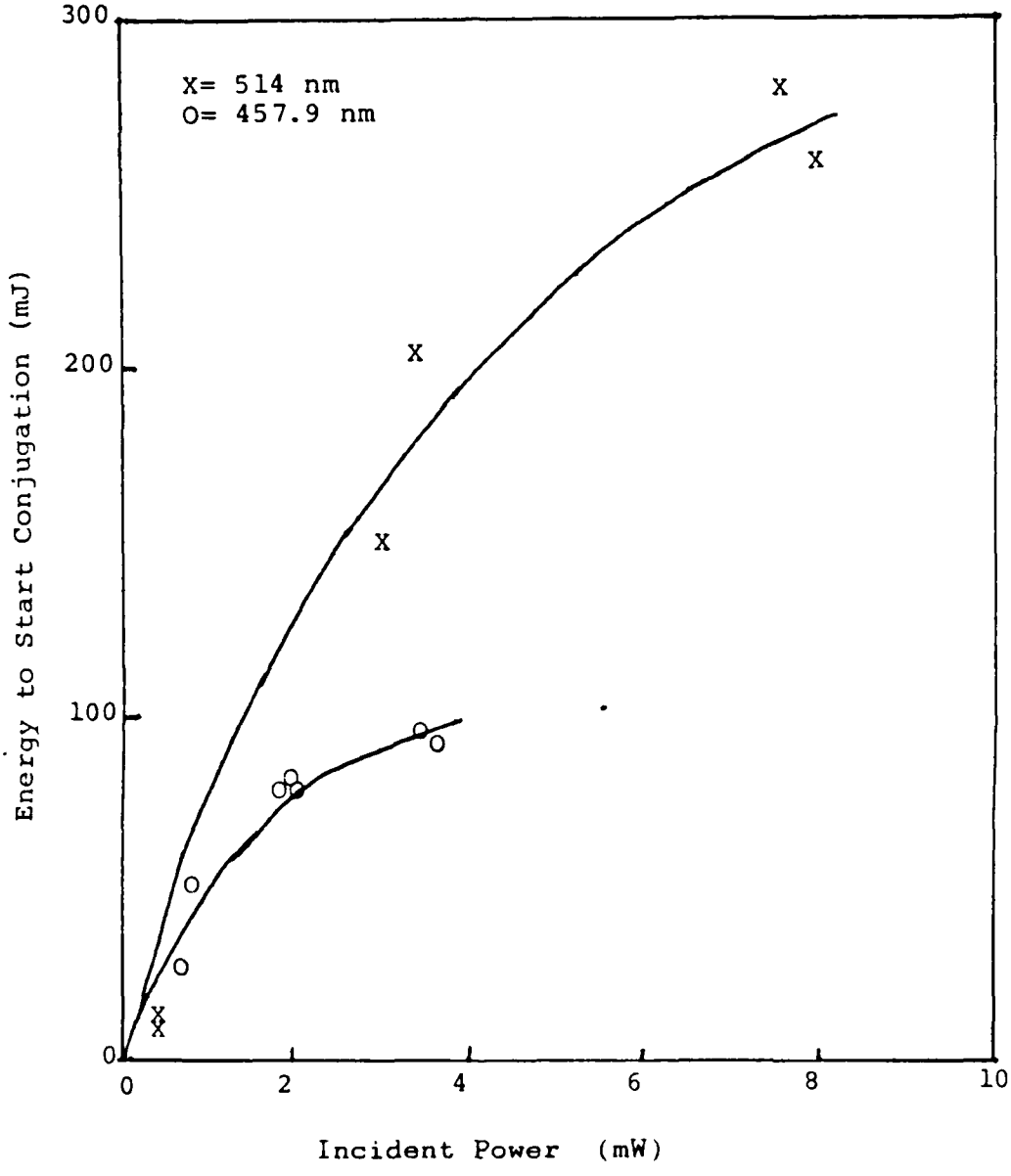

Figure 18. Energy to Start Conjugation as a Function of Incident Power, 25° Incident Angle

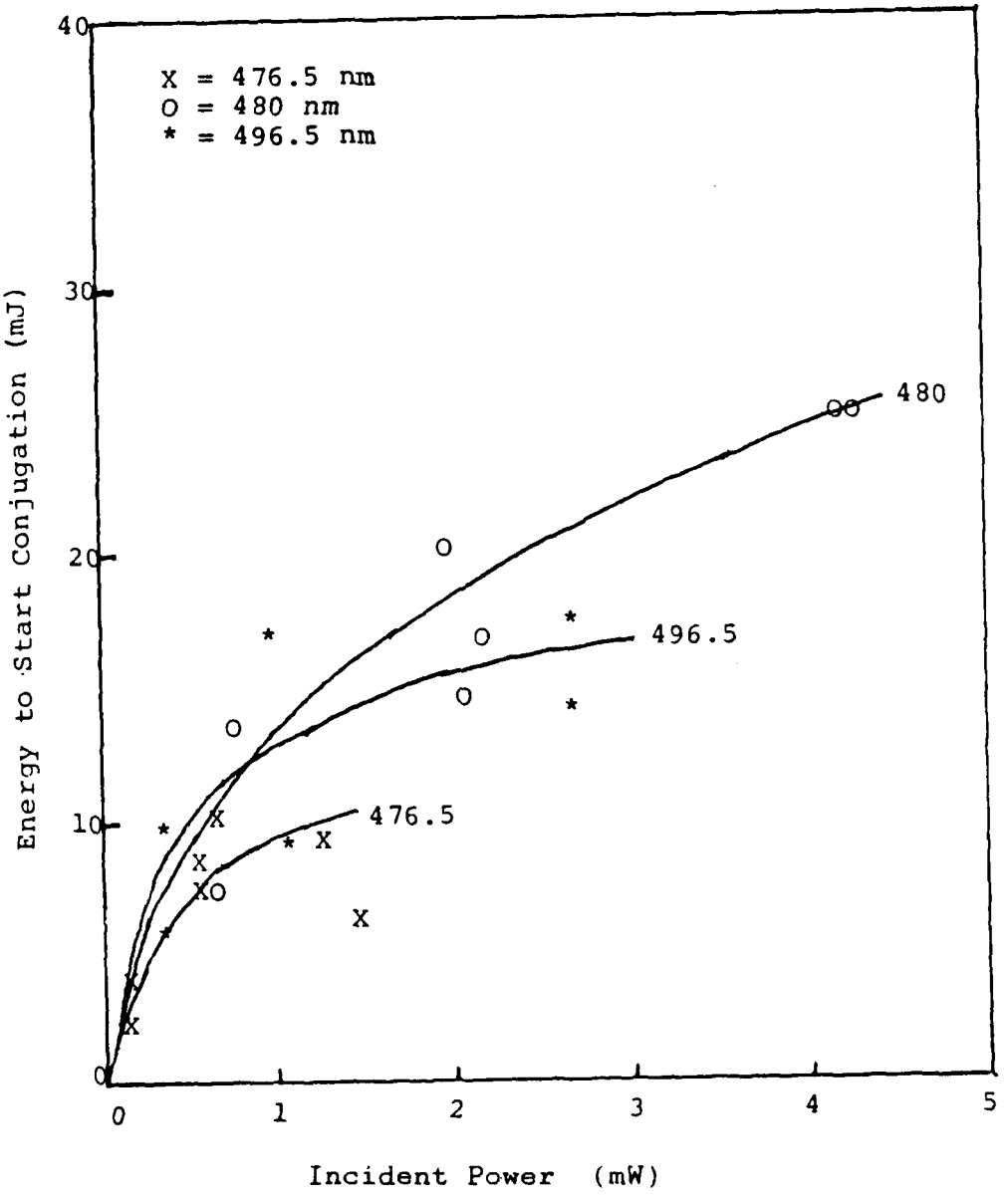

Figure 19. Energy to Start Conjugation as a Function of Incident Power, 25° Incident Angle

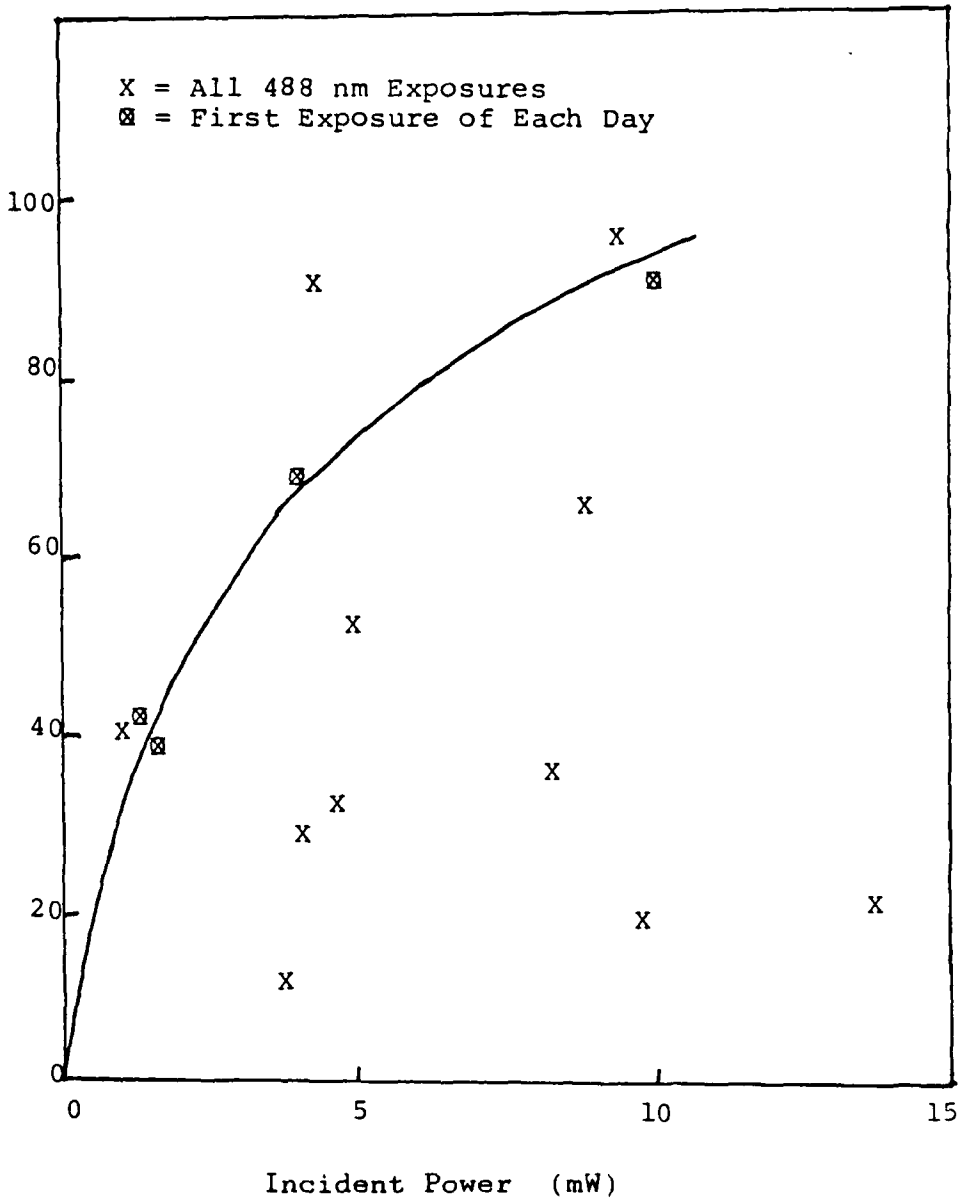

Figure 20. Energy to Start Conjugation as a Function of Incident Power, 25° Incident Angle

dependence on power. However, by plotting only the data taken during the first exposure of the crystal each day, a smooth curve was obtained. This indicates that in some cases part of the phase grating remained in the crystal after the ten minute waiting period, reducing the amount of energy needed to establish the subsequent grating. This line of the laser produced the highest power output, and the crystal showed the highest average phase conjugate returns for this frequency at any power. With more of a grating being established, it would take longer to decay. The 488 nm measurements were the first ones taken, and based on these results careful attention was paid to waiting a minimum of ten minutes between each subsequent measurement. The room lights were also turned on during the ten minutes so that the light would help erase the grating.

For each frequency, the amount of energy required to establish a grating increased with increasing power. The rate of increase was less than linear with power. A best fit to the curve for 514 nm gave the energy proportional to I^x with $x=0.52 \pm 0.15$. For 488 nm $x=0.34 \pm 0.08$, and for 457.9 nm $x=0.63 \pm 0.10$. Other frequencies had values for x in this range, but because of the limited range of power available for these low gain lines, extrapolation of a best fit curve was not as reliable. Those data points which were far below the others, indicating that the grating was not

completely erased prior to the measurement, were not included.

The average phase conjugate return as a percent of incident power was calculated, and as in the previous results, it was independent of power for each frequency. These results are shown in Figure 21. The highest return occurred for 488 nm, with 26.0%. If these results are corrected for the amount of light reflected off the face of the crystal, the values increase by 3%. Except for 457.9

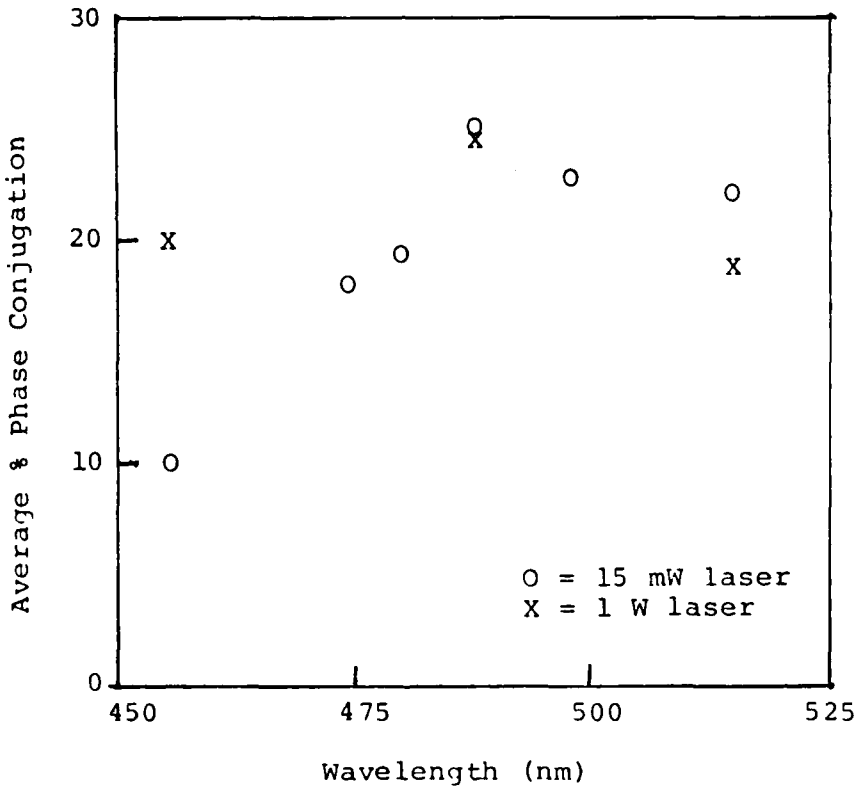

Figure 21. Average Percent Conjugate Return as a Function of Wavelength, 25° Incident Angle

nm, all values fell in the range of 18 to 26%. The lower value for 457.9 nm and the peak in response for 488 nm indicate that the crystal is most sensitive to the blue frequencies, or that the laser beam quality is poorer when it is off the peak line.

To determine if the choice of laser significantly affected the results, several measurements were made using a 1 W Argon ion laser. This laser was water cooled, and so did not have the vibration problem associated with the 15 mW laser. The time for a phase conjugate response to begin, and the final conjugate beam level, were recorded for 514, 488, and 457.9 nm. The phase conjugate beam as a percent of incident power is also shown in Figure 21. 488 nm produced the highest return (25%), and the return for 457.9 nm was now in the range corresponding to the other frequencies.

The diameter of the 1 W laser beam was approximately twice that of the 15 mW laser beam, and the 1 W laser could not be operated at powers as low as the other laser, so identical measurements could not be made for comparison. However, for each frequency the ratio of the energy to start phase conjugation in the 1 W laser, to the energy needed in the 15 mW laser, was the same. This indicated that the much higher value of energy required for 457.9 nm, which seemed out of line with the general downward trend in energy with increasing frequency, was not just an artifact of the laser.

IV. DISCUSSION OF RESULTS

A. PHASE CONJUGATE RETURN

Obtaining a phase conjugate return depended on having an extraordinary ray entering the barium titanate crystal to exploit the much larger r_{42} component of the electro-optic tensor. This involved polarizing the incident beam horizontally. Attempts to produce phase conjugation with a vertically polarized beam were unsuccessful.

The percent of phase conjugation was independent of power for a given frequency and angle of incidence with the c axis. Values recorded ranged from 10% for 457.9 nm, to 28% for 488 nm, which is in close agreement with published values of the expected range which are from 10 to 30%.

The phase conjugate beam exhibited the expected phase distortion correction properties, as evinced by the coupling of the beam back into the laser despite a large loss introduced by the Babinet compensator and quarter wave plate.

The phase grating could be established despite visible vibrations in the incident laser beam. When vibrations were present, the times required for phase conjugation to begin were erratic, and a conjugate beam did not always occur; but once established it would persist and would even itself vibrate on the detector. This demonstrates the rapid

adaptability of the phase grating in the crystal. However, displacements that did not allow the beam to hit the crystal in approximately the same spot as when the grating had been formed, erased the grating and several seconds were required to establish a new grating.

During use of the 1 W argon ion laser, a further demonstration of the phase conjugate properties was seen. As soon as the phase conjugate beam appeared (as measured by the return off the beamsplitter) the internal power of the laser started to increase, despite operation in a constant current mode. At 514 nm, a power increase of 500% was recorded. For 488 nm, power increased 175%, and at 457.9 nm, power increased 150%. The same Babinet compensator and quarter wave plate were used with the 1 W laser as had been used with the 15 mW laser. When the beam into the barium titanate crystal was blocked, the internal laser power immediately dropped to the initial values. It rapidly rose to the increased value when the beam was restored. The increase in laser power was compensated for in calculation of the percent phase conjugation, by measuring the power reflected off the beamsplitter concurrently with the measurement of the conjugate beam power.

The increase in power was caused by the conjugate beam travelling back into the laser cavity, and despite the losses along the path of propagation, causing the crystal to act as the end mirror for the cavity and increasing the

gain. To prevent this, a Faraday isolator between crossed polarizers should be used to isolate the returning conjugate beam from the laser. Since these are not commonly available, an alternative is to operate the 1 W laser at a high power level, and introduce a large loss (such as with a neutral density filter) so that the conjugate beam will be greatly attenuated before entering the laser. Further experiments on the effect of the conjugate beam on the mode structure of the laser should be performed.

B. GRATING PERSISTENCE MEASUREMENT

Initially, the grating decayed completely (i.e. to a level equivalent to leaving the crystal overnight) in ten minutes with no ambient light, after being established by a 5 mW beam, incident at an angle of 45° with the c axis. In subsequent measurements using higher powers and other angles, the grating persisted for even longer. The maximum value for the persistence of a grating in barium titanate crystals is given as 15 hours [Ref. 4: p. 214]. The time to full response for this crystal increased as the log of the interrupt time. Extrapolation of the response curve to an interrupt time of 15 hours, gives a time to full response as 95 seconds. None of the measurements were this long, so the dark current in this crystal is greater than the optimum value. Carefully flooding the crystal with room light for a full ten minutes erased the grating.

C. INCIDENT ANGLE RESPONSE

The optimum angles of incidence with the c axis for 488 nm were 25 and 45°. The reduced response between these values was not due to light reflected from the face of the crystal. One explanation for the unexpected maximum at 25° in Figure 15 is the geometry of the beam in the crystal. The threshold for self conjugation is $\beta l \geq 2.34$ with β given by equation 16. The optimum β occurs for α_2 5 to 10° less than α_1 [Ref. 13: p. 487]. For all angles, the incident beam was aligned for the center of the face of the crystal. Since the crystal is a cube, and the index of refraction is 2.4, α_1 is 69° and α_2 is 60° for an angle of incidence with the c axis of 25°. The difference between α_1 and α_2 is greater for larger angles of incidence with the c axis. This minimizes the amount of searching that must be done to find the corner. The two peaks in the response curve could then be due to competition between this effect and optimization of the direction of the resultant wave vector (generated by the sum of the two recording rays) with the c axis. Further experiments measuring the response at each angle as a function of the beam position along the back faces and corner will determine if the time for the beam to seek out the back corner is an important factor.

D. FREQUENCY RESPONSE

The energy required to establish a phase grating increased with increasing wavelength, in agreement with

theory, except for the 457.9 nm wavelength. This occurred for both lasers used, and therefore can not be attributed to excessive vibrations for this line of the 15 mW laser.

For each frequency, the increase in energy with power was less than linear, which agrees with the intensity dependence measured by Ducharme [Ref. 9]. The values of the intensity dependence were not the same for all frequencies, and did not exhibit a regular trend with increasing frequency. These last two results indicate that factors besides those measured influence the amount of phase conjugation. Further experiments measuring a wider range of powers and without feedback into the laser need to be performed.

E. OTHER OBSERVATIONS

Several phenomena occurred that were not expected, and which require further investigation. During grating persistence measurements of this crystal, the conjugate power for interrupt times between twenty seconds and two minutes, showed a dip in response after about two seconds. This might be due to interference between the incident beam and the diffracted beam from a partial grating.

At higher incident beam powers, the conjugate beam power overshot the steady state value, then decayed down in 5 to 10 seconds to the final value. The amount of overshoot varied with power and frequency, and was not always present. As previously described, the steady state value varied 4 to

8% due to feedback into the laser. These fluctuations were random with a 10 to 15 second period. In addition, the conjugate beam had a 15 ms periodic component. This is too fast to be due to 60 cycle interference. The source could be either a mechanical vibration of the laser cavity, a laser regulator response of some kind, or mode interactions inside the laser cavity. Investigation of these phenomena was outside the scope of the present work, and requires further experiments.

V. CONCLUSIONS

Optical phase conjugation was achieved through self-pumping in $BaTiO_3$ over a range in wavelengths from 457.9 to 514 nm. The average return amounted to about 25% of the incident beam. The phase conjugate return coupled back into the laser, affecting the laser modes. The process of phase conjugation was found to depend on the frequency, polarization, and angle of incidence of the incident beam. Obtaining a phase conjugate return required having an extraordinary ray enter the crystal. Angles of incidence with the c axis of 25 and 45° gave the maximum response. For each frequency, The energy to start conjugation depended on the incident intensity as I^x, with values of x from $x=0.34 \pm .08$ to $x=0.63 \pm .10$. Increasing the power at a given frequency did not affect the percentage of return, but did increase the speed of response. Vibrations that displaced the incident beam from its original position on the crystal adversely affected the process. Phenomena observed that warrant further investigation include: the S shaped response curve, the overshoot in conjugate response, the 4 to 8% drift in conjugate response, and the high speed fluctuations and 15 ms periodic component of the laser power when conjugate feedback is present.

LIST OF REFERENCES

1. Fisher,R.A., Introduction To and Application of Optical Phase Conjugation, paper presented at the Southwest Conference on Optics, Albuquerque, New Mexico,4 March 1985.

2. Yariv,A., Optical Electronics, CBS College Publishing, 1985.

3. Fisher,R.A., Optical Phase Conjugation, Academic Press Inc. 1983.

4. Gunter,P., "Holography, Coherent Light Amplification, and Optical Phase Conjugation With Photorefractive Materials," Physics Reports, v.93, pp. 199-299, 1982.

5. Klein,M.B., and Schwartz,R.N., "Photorefractive Effect in $BaTiO_3$: Microscopic Origins," J. Opt. Soc. Am. B, v.3, pp. 293-305, 1 February 1986.

6. Ducharme,S. and Feinberg,J., "Altering the Photorefractive Properties of $BaTiO_3$ By Reduction and Oxidation At 650° C," J. Opt. Soc. Am. B, v.3, pp. 283-292, 1 February 1986.

7. Feinberg,J., Heiman,D. Tanguay,A.R., and Hellwarth,R.W., "Photorefractive Effects and Light-induced Charge Migration in Barium Titanate," Journal of Applied Physics, v.51, pp. 1297-1305, 1 March 1980.

8. Kratzig,E., Welz,F., Orlowski,R., Doorman,V., and Rosenkrantz,M., "Holographic Storage Properties in $BaTiO_3$," Solid State Communications, v.34, pp. 817-820, 1985.

9. Ducharme,S. and Feinberg,J., "Speed of the Photorefractive Effect in a $BaTiO_3$ Single Crystal," Journal of Applied Physics, v.55, 1 July 1984.

10. Anderson,B.J., Forman,P.R., and Jahoda,F.C., "Self-pumped Phase Conjugation In $BaTiO_3$ At 1.06 μm," Optics Letters, v.5, pp. 627-628, 1 December 1985.

11. Chiou,A.E.T., and Pochi,Y., "Beam Cleanup Using Photorefractive Two-wave Mixing," Optics Letters, v.10, pp. 621, 1 December 1985.

12. Jahoda,F.C., Weber,P.G., and Feinberg,J., "Optical Feedback, Wavelength Response, and Interference Effects of Self-pumped Phase Conjugation in $BaTiO_3$," Optics Letters, v.9, pp. 362-364, 1 August 1984.

13. Feinberg,J., "Self-pumped, Continuous-wave Phase Conjugator Using Internal Reflection," Optics Letters, v.7, pp. 486-489, 1 October 1982.

14. Lam,L.K., Chang,T.Y., Feinberg,J., and Hellwarth,R.W., "Photorefractive-index Grating Formed By Nanosecond Optical Pulses in $BaTiO_3$," Optics Letters, v.6, pp. 475-477, 1 October 1981.

15. Chang,T.V., and Hellwarth,R.W., "Optical Phase Conjugation By Backscattering In Barium Titanate," Optics Letters, v.10, pp. 408-410, 1 August 1985.

INITIAL DISTRIBUTION LIST

		No. Copies
1.	Defense Technical Information Center Cameron Station Alexandria, Virginia 22304-6145	2
2.	Library, Code 0142 Naval Postgraduate School Monterey, California 93943-5002	2
3.	Prof. D.L. Walters, Code 61We Naval Postgraduate School Monterey, California 93943-5100	8
4.	Prof A.W. Cooper, Code 61Cr Naval Postgraduate School Monterey, California 93943-5100	1
5.	Prof. S. Baker, Code 61Ba Naval Postgraduate School Monterey, California 93943-5100	1
6.	Commanding Officer Attn: Lt. James R. Ryan Code 20 S.O.A.C. Naval Submarine School Box 700 Groton Ct 06349	2

END

DTIC

8-86